To the Graduate Council:

I am submitting herewith a thesis written by Heather Leigh McNabb entitled "Application of Calorimetric Testing and Dynamic Simulation to Predict and Control Violently Reactive Chemicals". I have examined the final copy of this thesis for form and content and recommend that it be accepted in partial fulfillment of the requirements for the degree of Master of Science, with a major in Chemical Engineering.

Dr. Charles F. Moore, Major Professor

We have read this thesis
and recommend its acceptance:

Accepted for the Council:

Interim Vice Provost and
Dean of the Graduate School

APPLICATION OF CALORIMETRIC TESTING AND DYNAMIC SIMULATION TO PREDICT AND CONTROL VIOLENTLY REACTIVE CHEMICAL REACTIONS

A Thesis
Presented for the
Master of Science
Degree
The University of Tennessee, Knoxville

Heather Leigh McNabb

December 2000

ACKNOWLEDGMENTS

I would like to express my appreciation to a number of individuals and groups for their support during my graduate education.

I thank Dr. Charlie Moore, my committee chairman, for his patience and guidance over the last several years. I also thank Drs. Frederick E. Weber and Duane D. Bruns for being willing to serve on my committee. I also thank Mrs. Carolina Hammond of the University of Tennessee's Distance Learning Program for her assistance and encouragement.

I thank Dr. Jim Downs, Mr. Peter Lodal, and Mr. Roland Patterson for their approval, support and supervision throughout my graduate studies. Jim believed in me and supported my decision to pursue a Masters Degree. Roland and Pete provided the subject content and resources to pursue this thesis. They also cleared huge hurdles to make possible the necessary research. Pete has been an enthusiastic supporter and has been a terrific mentor.

I thank Dr. Robert Clemens and Mr. Sam Ervin for their consideration and approval for the thesis topic.

I thank Drs. Ernie Vogel and Mike Paulonis and Mssrs. Ken Yount, H. David Miller, and John Cox as well as all the members of the Eastman Advanced Controls Technology group in Kingsport. Ernie, Mike, Ken and David have been invaluable resources for the application of dynamic simulation software. This work could not have been completed without their expertise in dynamic modeling. David and John were also wonderful study partners throughout my graduate courses and, through their own experiences, have helped guide the development of this thesis.

I also thank the research engineers, chemists and technicians who supported this work in the laboratory. Dr. David Olsen conducted the

bench-scale distillation testing and helped in deciphering the complex chemistry of the decomposition reactions. Mr. Curtis Teague conducted the Accelerated Rate Calorimetry Tests. Dr. Kent Morrill provided laboratory equipment and technicians to analyze the gas compositions. Mr. Jeff Smith of the Design Data Research Laboratory provided the physical property and vapor-liquid equilibrium data sets necessary for the computer simulations.

This work has been facilitated through the resources of Eastman Chemical Company, Tennessee Eastman Division, and I would like to express my appreciation to the management of the Worldwide Engineering & Construction Division and Operations Support Services Division for their support of this work.

I especially thank my husband, Kenney, who served as a technical editor for this report and has been a pillar of support throughout my graduate studies. He has persevered with me through countless days of exhaustion and frustration in my efforts to juggle school, work, and motherhood.

DEDICATION

This work is dedicated to my son, William Benjamin McNabb. His birth has brought new hope and joy in my life.

ABSTRACT

The purpose of this thesis is to demonstrate the use of calorimetric testing and dynamic simulation to predict and prevent the runaway reactions in a chemical process. A simple distillation process involving a complex runaway reaction is used to demonstrate this concept. An Accelerated Rate Calorimeter (ARC) is used to obtain reaction data (i.e. heats of reaction, reaction rates, reaction by-products, etc.). The reaction data is then used to develop a dynamic simulation of the distillation process for the purpose of evaluating failure scenarios that may trigger a runaway reaction. Finally, the simulator is used to assess the performance of different emergency safety systems (such as emergency shutdown systems, quench systems, dump systems, etc.) to prevent a potential runaway reaction.

Three failures scenarios (loss of cooling, loss of vacuum, and excess heat) are simulated in the refining process. The simulation results indicate that a typical emergency shutdown strategy (ESD) will prevent vessel over-pressurization in two of the three cases. For loss of vacuum, however, the emergency shutdown system, by itself, is ineffective for preventing vessel over-pressure. The simulation indicates that a reduction of the ESD initiation temperature and the addition of an emergency dump system can significantly reduce the potential for vessel over-pressurization.

TABLE OF CONTENTS

CHAPTER		PAGE
1	INTRODUCTION	1
2	LITERATURE REVIEW	5
	2.1 Diketene Decomposition	5
	2.2 Experimental Techniques to Characterize Runaway Reactions	7
	2.3 Interpreting Temperature Data from an Accelerated Rate Calorimeter	10
	2.4 Interpreting Pressure Data from an Rate Calorimeter	16
	2.5 Two-Phase Vapor-Liquid Flow Onset and Disengagement	19
3	LABORATORY ANALYSIS OF DIKETENE DECOMPOSITION	24
	3.1 Accelerated Rate Calorimeter Tests	24
	3.2 Bench-scale Distillation Tests	29
	3.3 Analysis of Diketene Decomposition Mechanism	30
4	DEVELOPMENT AND EVALUATION OF DECOMPOSITION MODEL USING DYNAMIC SIMULATION	33
	4.1 Development of Reaction Models	33
	4.2 Validation of Decomposition Model Using Dynamic Simulation	35
5	EVALUATION OF REFINING COLUMN SAFETY SYSTEMS USING DYNAMIC SIMULATION	47
	5.1 Process Description	47
	5.2 Simple Computer Model of Refining Column	48
	5.3 Emergency Shutdown System	51
	5.4 Evaluation of Failure Modes	53
	5.5 Discussion of Results	62
6	CONCLUSIONS AND RECOMMENDATIONS FOR FUTURE STUDY	64
	6.1 Conclusions	64
	6.2 Recommendations for Future Study	65

LIST OF REFERENCES 66

APPENDICES 68

A. DATA FOR REFINING COLUMN SIMULATION 69

VITA 75

LIST OF TABLES

TABLE		PAGE
3.1.	Initial Conditions for ARC Tests	24
3.2.	Summary Results from ARC Tests	25
3.3.	Calculated Values from ARC Test	27
3.4.	GC Mass Spec Analysis of Diketene Tars	30
4.1.	Estimated Number of Moles of CO2 Gas Generated by Diketene Decomposition	34
5.1.	Failure Analysis Summary for Refining Column Simulation	55

LIST OF FIGURES

FIGURE		PAGE
2.1	Diketene Molecular Structure (4-methyleneoxetan-2-one)	6
2.2.	Hydrolysis of Diketene	6
2.3.	Decomposition Mechanisms Proposed by Bianchi et al.	8
2.4.	Time-Temperature-Pressure Data from ARC Device	11
2.5.	Onset of Two-Phase Vapor-Liquid Flow in a Vessel	21
3.1.	Measured Temperature Rise for Diketene Decomposition in ARC Device	25
3.2.	Measured Pressure Rise for Diketene Decomposition Decomposition in ARC Device	26
3.3.	Log P versus Inverse Kelvin Temperature Data From Accelerated Rate Calorimeter Testing of Diketene	28
3.4.	Proposed Decomposition Mechanism for Diketene	32
4.1.	Proposed Reaction Models for Diketene Decomposition.	36
4.2.	Conceptual Representation of Computer Simulation of ARC Test	37
4.3.	Key Plan Indicating the Effect of Varying the Arrhenius Constant and Activation Energy in Dynamic Simulation of the Runaway Reaction of Diketene	39
4.4.	ARC Temperature Results Compared to Computer Simulation Using Proposed Reaction Mechanism #1 and Varying Activation Energy and Arrhenius Constants	39
4.5.	ARC Pressure Results Compared to Computer Simulation Using Proposed Reaction Mechanism #1 and Varying Activation Energy and Arrhenius Constants	40
4.6.	ARC Temperature Results Compared to Computer Simulation Using Proposed Reaction Mechanism #2 and Varying Activation Energy and Arrhenius Constants	41
4.7.	ARC Pressure Results Compared to Computer Simulation Using Proposed Reaction Mechanism #2 and Varying Activation Energy and Arrhenius Constants	41

4.8. ARC Self-Heat Rates Compared to Computer Simulation Using Proposed Reaction Mechanism #2..... 42

4.9. ARC Temperature Results Compared to Computer Simulation Using Proposed Reaction Mechanism #3 and Varying Activation Energy and Arrhenius Constants..... 42

4.10. ARC Pressure Results Compared to Computer Simulation Using Proposed Reaction Mechanism #3 and Varying Activation Energy and Arrhenius Constants..... 43

4.11. ARC Self-Heat Rates Compared to Computer Simulation Using Proposed Reaction Mechanism #3..... 43

4.12. ARC Temperature Results Compared to Computer Simulation Using Proposed Reaction Mechanism #4 and Varying Activation Energy and Arrhenius Constants..... 45

4.13. ARC Pressure Results Compared to Computer Simulation Using Proposed Reaction Mechanism #4 and Varying Activation Energy and Arrhenius Constants..... 45

4.14. ARC Self-Heat Rates Compared to Computer Simulation Using Proposed Reaction Mechanism #4..... 46

5.1 Refining Process for Crude Diketene..... 48

5.2 Conceptual Representation of Computer Model for Refining Column..... 50

5.3 Refining Simulation #1. The Change in the Temperature and Pressure in the Base of the Column After the Loss of Condenser Cooling and with only the ESD Active (Trip Temp. T1)..... 56

5.4 Refining Simulation #2. The Change in the Temperature and Pressure in the Base of the Column After the Loss of Condenser Cooling and with the ESD Active (Trip Temp. T1) and a 10 gpm Quench Stream..... 56

5.5 Refining Simulation #3. The Change in the Temperature and Pressure in the Base of the Column After the Loss of Condenser Cooling and with the ESD Active (Trip Temp. T1) and a 10 gpm Dump Stream..... 56

5.6 Refining Simulation #4. The Change in the Temperature and Pressure in the Base of the Column After the Loss of Condenser Cooling and with only The ESD Active (Trip Temp. T2) 57

5.7 Refining Simulation #5. The Change in the Temperature and Pressure in the Base of the Column

After the Loss of Vacuum and with only the ESD Active (Trip Temp. T1)..... 58

5.8 Refining Simulation #6. The Change in the Temperature and Pressure in the Base of the Column After the Loss of Vacuum and with the ESD Active (Trip Temp.) and a 10 gpm Quench Stream..... 58

5.9 Refining Simulation #7. The Change in the Temperature and Pressure in the Base of the Column After the Loss of Vacuum and with the ESD Active (Trip Temp. T1) and a 10 gpm Dump Stream..... 58

5.10 Refining Simulation #8. The Change in the Temperature and Pressure in the Base of the Column After the Loss of Vacuum and with only the ESD Active (Trip Temp. T2)..... 60

5.11 Refining Simulation #9. The Change in the Temperature and Pressure in the Base of the Column After the Loss of Vacuum and with the ESD Active (Trip Temp. T2) and a 10 gpm Quench Stream..... 60

5.12 Refining Simulation #10. The Change in the Temperature and Pressure in the Base of the Column After the Loss of Vacuum and with the ESD Active (Trip Temp. T2) and a 10 gpm Dump Stream..... 60

5.13 Refining Simulation #11. The Change in the Temperature and Pressure in the Base of the Column Upon Exposure to Excess Heat and with only the ESD Active (Trip Temp. T1)..... 61

5.14 Refining Simulation #12. The Change in the Temperature and Pressure in the Base of the Column Upon Exposure to Excess Heat and with only the ESD Active (Trip Temp. T2)..... 61

CHAPTER 1

INTRODUCTION

In the chemical process industry, there exist a few chemicals that have the potential to polymerize, decompose, or react violently. These highly energetic reactions, which are commonly referred to as "runaway reactions", may be initiated by the presence of another chemical, exposure to heat, or the passage of time. Chemicals that have the potential to runaway require special safety designs to provide for safe storage and handling.

Over the past 25 years, technology involved in the design of safety systems has markedly improved, enabling the prevention or mitigation of runaway reactions. One of the leading sponsors of the technology development is the Design Institute for Emergency Relief Systems (DIERS). Formed in 1976 under the auspices of the American Institute of Chemical Engineers (AIChE), this consortium of 29 companies has spent approximately $1.6 million to evaluate and develop pressure relief technology for runaway reactions (Fisher et al 1992). The DIERS research focuses on several areas including vapor disengagement dynamics, two-phase vapor-liquid flow models, calorimetric and vent testing, and computer simulations for relief and effluent design.

Despite the technological advancements in pressure relief systems, there are many cases in which the use of relief devices is not suitable for protection during a runaway reaction. For example, relief venting is ineffective when the reactants or products have insufficient heat of vaporization (i.e. non-condensable gases) to allow the venting process to temper the reaction. Relief venting is also undesirable when the release of reactants or products poses a significant explosive, ecological, or toxicological risk. Relief venting is impractical when very large relief devices, vent systems, and effluent handling systems are necessary. In such cases,

alternatives to relief venting, such as emergency shutdown systems, quenching, dumping, or inhibitor dosing to safeguard the process must be explored.

Dynamic simulation is a tool that can be used to explore these alternatives. With the appropriate reaction model, parametric studies can be performed which aid in determining which approach (i.e. prevention, quenching, dumping, or venting) is most effective for a particular process. Unfortunately, developing an exact model is often impossible due to the complexity of the chemical reaction. But with the development of improved calorimetric testing, it is now possible to develop behavioral models that can approximate the pressure-temperature behavior during a runaway. These behavioral models provide a practical means to evaluate safety systems for processes that historically have been difficult to control.

Traditionally, differential thermal scanning (DSC) or thermogravimetry (TG) have been used to determine whether or not the potential exists for a runaway reaction and to quantify the heat of reaction and reaction kinetics. These inexpensive tests are usually requested either as part of a forensic investigation following an accident or as a screening tool for new and existing processes. Unfortunately, these two calorimetric devices have a common weakness. They fail to characterize the rise in pressure resulting from the formation of vapors and/or non-condensable gases.

In the 1970s, researchers in the laboratories of DOW Chemical Company developed the Accelerated Rate Calorimeter (ARC). This device can provide both temperature and pressure data during a runaway reaction. This data can then be used to characterize the runaway reaction and to estimate kinetic parameters, heat of reaction, and self-heat rates.

As demonstrated in this thesis, a simple behavior model of a runaway reaction can be developed from ARC testing. Although the model does not accurately describe the chemical composition, it does adequately

predict the temperature, pressure, and energy behavior within a specified range of process conditions. Therefore, the model can be used successfully to dynamically simulate the chemical process and evaluate design and control options that may prevent and or mitigate a runaway reaction.

A simple distillation column involving a hypothetical runaway reaction of diketene is used to demonstrate this concept. Diketene is an intermediate chemical used in the production of acetoacetate esters and acetoamides. It is typically manufactured from the pyrolysis of acetic acid to form ketene and then subsequent dimerization of the monomer. The last processing step usually involves the purification of diketene by vacuum distillation.

When pure diketene is exposed to elevated temperatures, it can decompose violently. Despite this potential for decomposition, diketene has been produced safely in the chemical process industry for more than half a century with no major incidences or losses reportedly caused by a decomposition reaction.

Diketene is, however, a strong lachrymator and if released, may cause respiratory distress or pulmonary edema to persons exposed. It is also flammable and readily ignites. Consequently, a release of diketene liquid or vapor is undesirable. The manufacture of diketene is, therefore, a case in point that clearly illustrates the importance of prevention rather than mitigation (i.e. emergency relief venting) of a runaway reaction. With a history of safe operation and readily available information regarding the manufacture of diketene and decomposition reaction, the refining of diketene is a suitable candidate to demonstrate the application of calorimetric testing and dynamic simulation to predict, prevent, and control runaway reactions.

In this work, the mechanism by which diketene decomposes is explored through laboratory testing. An Accelerated Rate Calorimeter (ARC) is used to characterize the reaction and provide preliminary estimates

for reaction kinetics. From the ARC data, various behavioral reaction models are proposed and evaluated by means of a computer simulation. A suitable behavioral model is selected and used as the basis for developing a simulator of a typical diketene refining process. The simulator is then used to compare and evaluate various representative emergency response strategies that may be implemented for a process involving a runaway reaction.

CHAPTER 2

LITERATURE REVIEW

2.1 Diketene Decomposition

For commercial quantities, diketene is produced in a three-step process. In the first step, ketene is formed from the pyrolysis of acetic acid, acetic anhydride, or acetone. The ketene then dimerizes to form crude diketene. In the last step, vacuum distillation is used to purify the crude product.

At room temperature, diketene is a colorless liquid with a molecular weight of 84.07 g/mol and a density slightly above that of water (1.09 g/ml). Its atmospheric boiling point, 127°C, is also above that of water.

Diketene requires special care in handling and storage. It is a strong lachrymator and can cause severe burns to the eyes, skin, and respiratory tract. Exposure to the eyes can damage corneal tissue. The formation of pulmonary edema is also possible up to 2 days after exposure (Miller et al 1990). Diketene is also a flammable liquid with a flashpoint of 34°C (93°F) and is highly reactive in the presence of acids, bases, amines, oxidizers, Friedel-Craft catalysts, and water. Diketene is thermally unstable and can violently decompose at temperatures above 98°C. (Agreda and Zoeller 1993). For these reasons, bulk transportation of diketene is prohibited in many countries.

Nevertheless, the very reactive nature of diketene is the reason it is a versatile and effective chemical intermediate. It is primarily used for the commercial production of acetoacetate esters and acetoamides. The high reactivity of the diketene molecule can be attributed to its unsaturated structure (see Figure 2.1) and strained four-membered heterocyclic ring (E_{strain} ~ 22.5 kcal/mol) (Agreda and Zoeller 1993).

For this reason, most reactions with diketene are "ring opening" and exothermic in nature. Although, there are a few published diketene reactions in which the β-lactone ring remains intact. These few exceptions typically occur under free-radical conditions (Clemens 1986; Miller et al 1990).

When exposed to water, diketene slowly hydrolyzes to form the intermediate compound, acetoacetic acid. The intermediate acid, in turn, rapidly decomposes into acetone and carbon dioxide (see Figure 2.2). The heat of reaction for hydrolysis at 25°C is calculated as -29.34 kcal/gmol (Perry's 1984; Mansson et al 1968).

At room temperature, liquid diketene slowly self-condenses to form dimers, oligomers, and polymers. The most common condensation product is the diketene dimer, dehydroacetic acid (molecular weight 168 g/mol) (Clemens 1986). At elevated temperatures, the decomposition of diketene proceeds rapidly and liberates 0.5 moles of gas per mole of

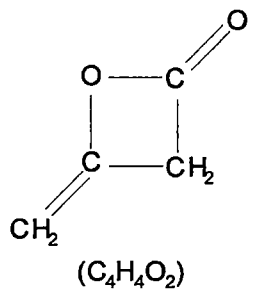

Figure 2.1: Diketene Molecular Structure (4-methyleneoxetan-2-one)

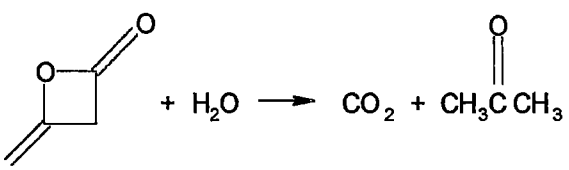

Figure 2.2: Hydrolysis of Diketene.

diketene consumed (Fuller 1984). In the presence of strong acids or bases, diketene can self-condense or polymerize violently.

The decomposition of diketene is very exothermic and liberates ~90 kJ/gmol of energy (Bianchi et al 1985; Lopatin et al 1992). The reported temperature at which diketene decomposes (i.e. the self-accelerating decomposition temperature "SADT") varies in the industry literature. In most publications, the reported SADT is between 98°C to 125°C (Fuller 1984; Bianchi et al 1985; Agreda and Zoeller 1993). Some articles, however, report the SADT as low as 62°C (Lopatin et al 1992).

The reason for the reported differences in SADT is not clear. Bianchi et al (1985) suggest that the presence of acetic acid, a common impurity in diketene, has a pronounced effect on the SADT. They observed that increasing quantities of acetic acid significantly reduced the initiation temperature. They also observed that the pressure rise during the runaway was substantially less with increasing quantities of acetic acid. They concluded, therefore, that diketene decomposes by way of two possible reactions (see Figure 2.3), each with different activation energies. Under the conditions imposed in their experimentation, the activation energies were estimated as 72 kJ/mol for Reaction (a) and 104 kJ/mol for Reaction (b).

2.2 Experimental Techniques to Characterize Runaway Reactions

A differential scanning calorimeter (DSC) is commonly used to screen chemicals for runaway reactions. This device can be used to obtain heat of reaction data with reasonable accuracy from small samples (~10 mg). But because of its lack of sensitivity, DSC can only provide approximations for the reaction rate data and self-acceleration decomposition temperature. Furthermore, DSC cannot provide time-dependent pressure data during a runaway reaction. For this reason, DSC testing cannot adequately characterize a runaway reaction.

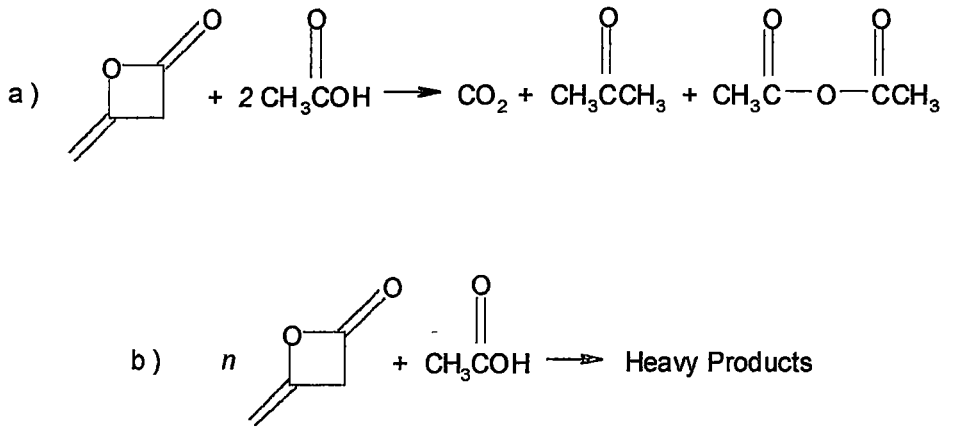

Figure 2.3: Decomposition Mechanisms Proposed by Bianchi et al.

To provide better information on runaway reactions, the members and contractors of the Design Institute of Emergency Relief Systems (DIERS) developed several new calorimeters. The first of these, the Accelerating Rate Calorimeter (ARC), was developed in the laboratories of Dow Chemical Company. The ARC device offers several advantages over DSC. DSC is limited to small sample sizes (~10 mg) but the ARC can accommodate larger samples (~10 g) in its sample bomb. The ARC also provides temperature and pressure data and is very sensitive over a wide range of temperatures. It can measure exotherms as low as 0.02°C/min (Becker et al 1998) and maintain near adiabatic conditions for self-heat rates up to 15°C/min. The ARC device is fully automated and requires very little operator attention. The data generated by the ARC can be used to develop reaction kinetics, however, the data cannot be used to directly infer the safety of a particular process.

The primary disadvantage of the ARC device is the relatively high thermal inertia of the sample container. This creates both a lag in the temperature measurement and biases the maximum adiabatic temperature rise. For this reason, the data obtained from an ARC test is not directly applicable to most commercial chemical processes in which the thermal inertia of the reaction vessel is relatively low.

The ARC data, therefore, must be scaled using a compensating factor known as the ϕ-factor. The effect of the thermal inertia is discussed in more detail in Section 2.3.

Another disadvantage of the ARC device is that the data is obtained from a closed system. The ARC device, therefore, cannot provide vapor liquid disengagement data, foaming or frothing characteristics, nor two-phase vapor-liquid flow information. Such data is necessary in order to accurately size relief devices for runaway reactions. Nor can the ARC reproduce the dynamic effects in a real process such as the effects of influent or effluent streams, process coolers or heaters, emergency shutdown systems, etc. Despite these disadvantages, the ARC test is still commonly used in the chemical industry because of its moderate cost and ease of use.

Fauske and Associates, Inc. commercialized two other calorimeters for use in characterizing runaway reactions. The first is the DIERS bench scale apparatus, which is marketed as the Vent Sizing Package (VSP2™). This device can be operated in either a closed or vented system. When operated in the closed system mode, the VSP2™ uses nitrogen gas pressure to compensate for the weak-walled test cell. In the vented mode, the contents of the test cell are vented into a secondary containment vessel. The 120 ml test cell has very low thermal inertia ($\phi \approx 1.05$) (Fauske et al 1986) as compared to that of the ARC device ($1.5 < \phi < 6$) (Fisher et al 1982). Temperature lags are avoided by measuring the sample temperature directly. The disadvantages of the VSP2™ are the equipment cost, the required level of operator care and attention, and cleaning requirements following each test.

The Relief Size Screening Tool (RSST™) is also a vented test system with low thermal inertia. The RSST™ uses a small, 10-ml glass test cell of low heat capacity (Becker et al, 1992), but offers few other advantages over the VSP2™.

2.3 Interpreting Temperature Data from an Accelerated Rate Calorimeter.

The operating principle of the ARC device is simple. The sample is placed in a 10 ml titanium spherical test vessel and a pressure transmitter is mounted at the throat to seal the unit. The sealed test vessel is commonly called a "bomb". The term "bomb" is misleading. The name refers only to the fact that the container is a heated pressure vessel and does not imply any explosive behavior of the material therein. The bomb is then placed inside a protective jacket containing radiant heaters. Two thermocouples are connected, one to the outside surface of the bomb and the other to the inside surface of the jacket. A microprocessor monitors the temperatures and pressure and controls the heat input by adjusting the radiant heaters.

At the start of the test, a microprocessor raises the bomb temperature slowly through a series of heat and wait steps. An exotherm is detected when the temperature at the bomb surface begins to increase at a rate (> 0.02 °C/min) during the "wait" step. The control system manipulates the radiant heaters to maintain the temperature between the heater and the bomb surface equal to the temperature measured at the bomb surface. This ensures adiabatic conditions for the bomb. The control system records the pressure and temperature changes over time and provides this data graphically. An example of ARC data is shown in Figure 2.4.

The kinetic parameters such as reaction order, the reaction rate, and the heat of reaction can be determined from the temperature data. Townsend and Tou (1980) discuss in detail the techniques used to determine the kinetic parameters. For a single component reaction with a reaction order n and maintained under adiabatic conditions, the composition can be defined by fractional temperature rise for a given initial composition. This means that at any time (t) or temperature (T), the concentration can be approximated by the equation,

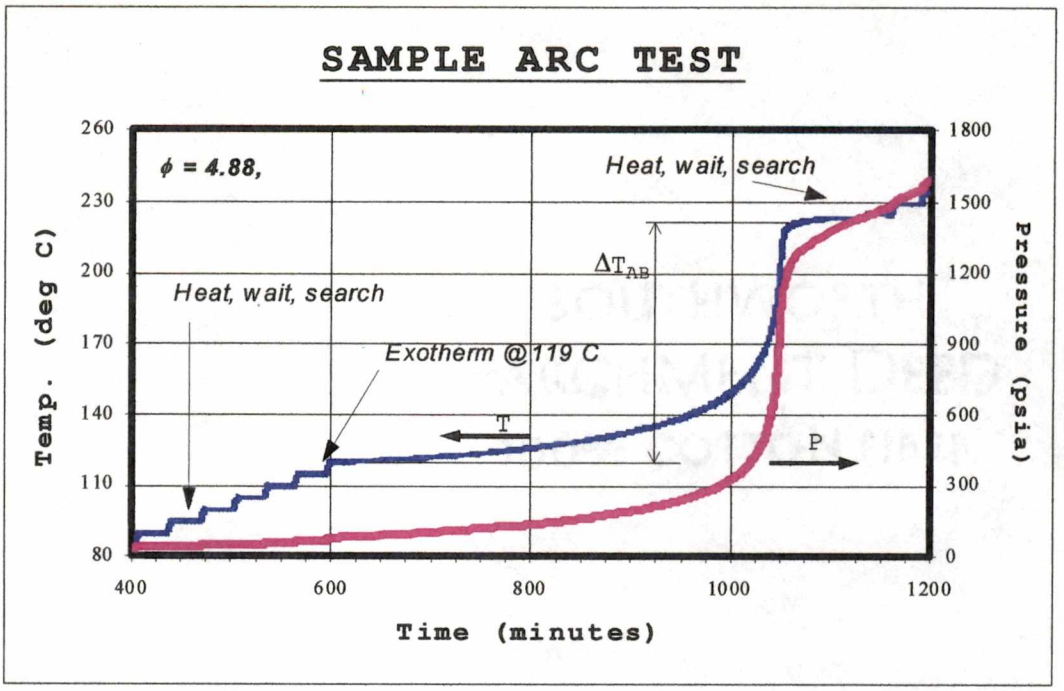

Figure 2.4: Time-Temperature-Pressure Data from ARC Device.

$$C = \frac{T_f - T}{\Delta T_{AB}} C_o$$

where T_f is the final temperature after the exotherm, ĆT_{AB} is the adiabatic temperature rise (T_f - T_o), and C_o is the initial concentration. By substituting the above expression into the Power Law rate equation, $dC/dt = -kC^n$, and differentiating with respect to T, the kinetic event can be related to the sample temperature by

$$\frac{dT}{dt} = k\left(\frac{T_f - T}{\Delta T_{AB}}\right)^n \Delta T_{AB} C_o^{n-1}$$

where k is the Arrhenius expression, $k=Ae^{E/RT}$. The term dT/dt is referred to as the self-heat rate. The temperature at the maximum self-heat rate, T_m, can be determined by evaluating the above expression where $d^2T/dt^2=0$.

Townsend and Tou (1980) also show that the pseudo rate constant, k^*, is related to the temperature by the equation,

$$\ln k^* = \ln C_o^{n-1} A - \frac{E}{R}\left(\frac{1}{T}\right)$$

where $k^* = C_o^{n-1} k$. The order of the reaction, n, and the Arrhenius parameters, E and A, are evaluated by plotting $\ln k^*$ vs. 1/T. When the reaction order is correctly chosen, the plot produces a straight line and the parameters, E and A, can be calculated directly from slope and intercept.

The heat of reaction is determined by the equation

$$\Delta H_r = M\overline{C}_v \Delta T_{AB}$$

where M is the mass and $\overline{C}_v$ is the average heat capacity of the sample over the temperature range of the exotherm.

The previous equations are based upon the assumption that the sample is maintained at adiabatic conditions. Within the ARC device, the bomb is maintained under adiabatic conditions, but not the sample. Because of the high thermal inertia of the test vessel, the sample actually looses energy to heat the bomb. The fraction of energy retained in the sample at any instant is referred to as the "degree of adiabaticity" and is given the symbol "a". The adiabaticity of the sample and thermal inertia of the bomb are thus inversely proportional.

The high thermal inertia creates both a lag in the temperature measurement and biases the maximum adiabatic temperature rise of the sample. Consequently, the measured temperature and pressure must be corrected before any of the previous equations can be applied. A simple correction factor is used to adjust the maximum adiabatic

temperature rise. This factor, known as the ϕ-factor, is derived from the energy balance as follows

$$M\overline{C}_v\Delta T_{AB} = (M\overline{C}_v + M_b\overline{C}_{vb})\Delta T_{AB,s}$$

where:
- M = mass of the sample
- $\overline{C}_v$ = heat capacity of the sample
- ΔT_{AB} = theoretical adiabatic heat rise of sample (i.e. if no energy were lost to the bomb)
- M_b = mass of the bomb
- $\overline{C}_{vb}$ = heat capacity of the bomb, and
- $\Delta T_{AB,s}$ = measured adiabatic heat rise of the bomb and the sample.

By rearranging the previous equation, the corrected value of the maximum adiabatic temperature rise is

$$\Delta T_{AB} = \phi\Delta T_{AB,s}$$

where,

$$\phi = 1 + \frac{M_b\overline{C}_{vb}}{M\overline{C}_v}.$$

Values of the ϕ-factor for the ARC device typically vary from 1.5 to 6.0 (Fisher et al 1982). A ϕ-factor of 2 implies that half of the reaction energy is used to sensibly heat the bomb or reaction vessel. But, in most commercial chemical processes, the mass of the reaction vessel is usually small compared to the contents therein. Hence, the thermal inertia of the commercial vessel is usually negligible and the ϕ-factor is approximately unity ($\phi \approx 1$). Consequently, the same reaction occurring in a commercial process vessel may exhibit a faster self-heat rate (dT/dt) and reach a higher maximum temperature (T_m) than is observed in the ARC test ($\phi > 1$).

The "degree of adiabaticity" and the ϕ-factor are exact mathematical inverses for conditions of equal rates of change of the bomb wall and sample temperatures. But because of the appreciable thermal inertia of the bomb, the temperature of the sample (T_r) actually rises at a rate faster than is measured by the thermocouple on the outside of the bomb wall (T_w). The sample temperature at any time, t, is thus determined from the heat flux ($q=hA\acute{C}T$) from the sample itself to the bomb wall. Neglecting the heat loss to the air space and the thermowell and assuming that the fraction of material vaporized is small, then Huff (1982) shows that

$$T_r - T_w = \Lambda_w (dT_w/dt)$$

where: dT_w/dt = self-heat rate of bomb wall, °C/sec

Λ_w = heat transfer parameter of the wall, seconds

= $M_b C_{vb}/hA$

For a standard 9-ml ARC sample bomb that is half-full of non-viscous liquid, the heat transfer parameter can be estimated by $\Lambda_w = 2.9 M_b C_{vb}$, where Λ_w in seconds and $M_b C_{vb}$ is in J/°K (Huff 1982).

Once the sample temperature has been adjusted for the time lag, the self-heat rate of the sample (dT_r/dt) at any point in time is easily calculated as the slope of the curve, T_r vs. Time.

The adiabaticity can also be calculated from the heat balance. Neglecting heat losses to the thermowell and air space, the adiabaticity is derived by Huff (1982) as

$$a = \left\{ 1 + \frac{M_b \overline{C}_{vb} (dT_w/dt)}{M \overline{C}_v (dT_r/dt)} \right\}^{-1} .$$

Lastly, if the adiabaticity under the test conditions is known, the temperature and the self-heat rate (dT_r/dt) of the sample can be determined at any other adiabaticity (a=1 for example) provided the

compositions are the same in both cases. The key is the previous assumption that the composition is defined by fractional temperature rise for a given initial composition. Then for the same composition (C/C_o), it can be shown that the temperature and adiabaticity are related as follows,

$$(T_f - T)_{a=1} = \frac{1}{a}(T_f - T)_a .$$

The temperature terms shown in the previous equation are written in the general sense. They can represent wall temperatures (T_w) or sample temperatures (T_r).

Huff (1982) also develops the following equation to predict the self-heat rate under conditions of a=1,

$$\frac{(dT_r/dt)_{a=1}}{(dT_r/dt)} = \frac{1}{a}\exp\left\{-\frac{E}{R}\left(\frac{1}{T_{r,a=1}} + \frac{1}{T_r}\right)\right\}$$

for reactions limited to the following conditions:

1. The reaction rate can be represented by a Power Law rate expression over the temperature range of interest.
2. The apparent activation energy, E, varies only slightly over the temperature and composition range of interest.
3. For a given initial composition, the extent of conversion is defined by a fixed function.
4. The extent of chemical reaction at any temperature is defined by the extent of temperature rise with respect to the final rise, regardless of the temperature level.

For simple exothermic reactions, the ARC test can provide reasonable kinetic parameters. However, if the reaction mechanism is very complex (e.g. parallel reactions) or the reaction mechanism changes over the temperature range such that simple Power Law behavior is not

observed, the kinetic parameter estimates not valid. Furthermore, if the thermal inertia, ϕ, greatly exceeds 6, or the self-heat rate exceeds 15°C/min then the test results should be questioned.

With the advent of powerful computers, manual computation is seldom necessary. Automated programs quickly provide the corrections for thermal inertia and provide estimates for the kinetic parameters. The equations presented within this section, therefore, are provided to assist in understanding the theory behind the Accelerated Rate Calorimeter and to provide necessary insight into the limitations of its use.

2.4 Interpreting Pressure Data from an Accelerated Rate Calorimeter.

The pressure data from an ARC test is necessary to characterize whether the reaction is *volatile*, *gassy*, or *hybrid* and whether the reaction is *tempered* or *non-tempered*. A *volatile* reaction is one in which the reactants, products, and/or solvents have sufficient volatility and heat of vaporization such that if the vessel is properly vented, vaporization would maintain or even cool the reaction. *Volatile* reactions, by definition, are *tempered*. On the other extreme, *Gassy* reactions are *non-tempered*. As the name implies, *gassy* reactions result from decompositions that form non-condensable gases. The reactants, other by-products, and/or solvents in the system have either insufficient volatility or such low heat of vaporization that venting cannot cool the reaction. *Hybrid* reactions have both condensable and non-condensable components. Therefore, hybrid reactions can be either *tempered* or *non-tempered* depending on the volatility, quantity, and heat of vaporization of the reactants, products, and/or solvents.

Volatile, gassy, and hybrid reactions are easily distinguished by plotting ln P vs. -1/T data generated from the closed system ARC test (Becker et al 1998). For volatile systems, ln P increases linearly

with increasing temperature, as is characteristic of vapor pressure plots. In contrast, gassy systems exhibit small increases in ln P at the beginning and end of the reaction when the pressure is solely a function of the gas laws. But at temperatures near the peak reaction (T_m), there is an exponential rise in ln P. This corresponds to the rapid formation of gas molecules. The log plot for a hybrid reaction will exhibit both linear (at the beginning and end) and exponential behavior (near T_m).

The type of reaction system can be inferred from the log plots of the measured or "raw" pressure data. However, the pressure in the bomb is a function of the sample temperature as well as the total number of moles of gas/vapor and the volume of the vessel. Since the temperature increase of the sample is diminished by the thermal inertia, the pressure rise is also diminished. Consequently, the measured pressures must be corrected before they can be used to calculate vapor or gas generation rates.

The pressure correction is achieved by assuming that the vapor and liquid phases are in thermodynamic equilibrium throughout the runaway. Therefore, the sample temperature is first corrected for the adiabaticity, then the correct pressure is calculated from phase equilibria. The concept is fundamentally simple but the calculations may be highly complex when non-ideal gases and liquids are present.

Huff (1982) uses a simple styrene polymerization to demonstrate the pressure and temperature correction for adiabatic conditions (a=1) from data measured by the ARC ($a_{obs} < 1$). An abbreviated version of Huff's discussion is presented in the following paragraphs.

Consider a liquid mixture in equilibrium with an ideal gas (i.e. the fugacity equals the partial pressure). The total pressure is, therefore, the sum of the partial pressures,

$$P = \Sigma p_i .$$

The partial pressures of the condensable components given by

$$p_i = x_i \gamma_i P_i^o ,$$

where x_i is the liquid mole fraction, γ_i is the liquid activity coefficient, and P_i^o is the vapor pressure of component i. For many chemicals, the vapor pressures may be calculated from Antoine's Equation

$$\log_{10}(P_i^o) = A_i - B_i/(T - 273.2 + C_i)$$

over the temperature range of interest.

The non-condensable gases are usually treated separately from the condensable vapors. The total pressure of the system is adjusted by subtracting the partial pressure of the non-condensable gas pad above the sample. Assuming the change in vapor volume is negligible and the ideal gas relation $p_g = T(p_g/T)^\circ$ holds, then the adjusted pressure, $P' = P - p_g$.

The adjusted total pressure can then be expressed in terms of Antoine's equation,

$$P' = \Sigma(x_i \gamma_i) 10^{[A_i - B_i/(T - 273.2 + C_i)]} .$$

When components are similar in nature, average values of B_i and C_i can often be used to represent all components in the temperature range of interest without a significant decline in accuracy. This is also a reasonable assumption in the case where one component dominates the behavior of the mixture. Therefore, the previous equation reduces to

$$P' = (F') 10^{[-\bar{B}/(T - 273.2 + \bar{C})]} ,$$

where

$$F' = \Sigma(x_i \gamma_i) 10^{[A_i]}.$$

The function F′ is strongly dependent on composition and weakly dependent on temperature. When the composition is fixed, the function F′ is approximately constant. Therefore, the following relationship can be derived to predict the sample pressure that would be observed in a truly adiabatic system.

$$\log_{10}\left(\frac{P'_{a=1}}{P'}\right) = \overline{B}\left[\frac{1}{T_r - 273.2 + \overline{C}} - \frac{1}{T_{r,a=1} - 273.2 + \overline{C}}\right]$$

In this case, P' is the total pressure measured during the ARC test less the partial pressure of the initial gas pad and T_r is the sample temperature as defined in Section 2.3.

For cases where the vapor-liquid equilibrium is highly non-ideal or where the number of non-condensable gas moles changes as the reaction progresses, the pressure correction models become computationally difficult. Computer models become necessary to predict the pressure under low thermal inertia conditions.

2.5 Two-Phase Vapor-Liquid Flow Onset and Disengagement

For highly energetic runaway reactions, the rate of vapor or gas generation can be so violent that vapor-liquid disengagement is limited. Boiling occurs throughout the liquid, not just at the liquid surface. Partial disengagement or vapor entrainment may cause the reaction mixture to foam, froth, or swell.

The Design Institute of Emergency Relief Systems (DIERS) has spent a great deal of time and money studying two-phase fluid behavior as it relates to relief device sizing and computer simulation. DIERS evaluated various fluid dynamic models in two areas: (a) vapor-liquid disengagement within the vessel and (b) two-phase vapor-liquid flow in

nozzles and pipes. The maximum two-phase volumetric flow rate (i.e. choke flow) through a nozzle or pipe is generally much less than can be attained by single-phase liquid or vapor flow. Consequently, systems prone to two-phase flow require much larger relief and vent areas.

The possibility of two-phase flow must be considered anytime a runaway reaction system is modeled. The person or persons who model the process must understand the conditions that ensure disengagement and/or predict the onset of two-phase vapor-liquid flow. For this reason, a brief summary of the method to predict the onset of two-phase vapor-liquid is provided herein.

Liquid swell in a vessel is a function of the bubble "slip". Bubble slip, however, is dependent on many parameters including liquid and vapor densities, liquid viscosity, buoyancy, surface tension, the vapor void fraction, and the foaming potential for the liquid. Very viscous or foamy liquids easily trap gas molecules and tend towards greater liquid swell. Two-phase flow often occurs when venting viscous or foamy fluids.

For non-viscous or non-foamy liquids, two phase venting will arise if and only if the liquid inventory is above a minimum threshold and if the vapor flux is sufficient to swell the aerated liquid to the mouth of the effluent or vent pipe (see Figure 2.5) (Becker et al 1998).

The three most commonly used two-phase vapor-liquid onset and disengagement models are the (a) Homogenous (no slip) effluent, (b) Churn-Turbulent effluent and (c) Bubbly Vessel effluent.

The Homogenous effluent model assumes no "slip" and, consequently, no disengagement between the vapor and liquid molecules. Vapor droplets are small, uniformly distributed throughout the liquid, and have large surface-to-volume ratios. The viscous drag forces are large compared to the buoyant forces. Therefore, the vapor rise velocity (U_∞)

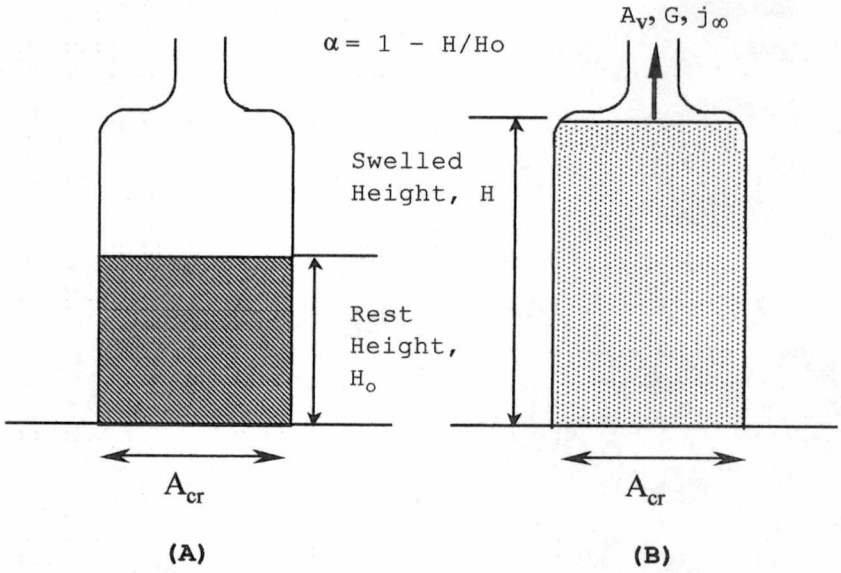

Figure 2.5: Onset of Vapor-Liquid Two-Phase Flow in a Vessel
(A) Liquid at rest in open vessel;
(B) Liquid swell from gas holdup

relative to the liquid (Fisher et al 1982) is zero. This model is usually reserved for very viscous or foamy fluids.

Churn-Turbulent and Bubbly Vessel Models are both based on the assumption of partial disengagement of vapor and liquid. The bubbles can "slip" through the liquid and can coalesce to form larger bubbles. The bubble rise velocity (U_∞) relative to the liquid in a cylindrical vessel can be calculated by the general equation

$$U_\infty = K \frac{\sqrt[4]{\sigma g(\rho_f - \rho_g)}}{\sqrt{\rho_f}}$$

where σ = Surface tension of liquid,
ρ_f = Liquid density, and
ρ_g = Vapor density.

The constant, K is determined empirically. For Churn-Turbulent systems, K = 1.53. For Bubbly Vessels, K = 1.18 (Becker et al 1998).

The superficial vapor velocity ($J_{g\infty}$) is the volumetric vapor flow rate per unit cross sectional area of the vessel. The dimensionless superficial vapor velocity (B_f) is defined as the ratio of the superficial vapor and bubble rise velocities. For Churn-Turbulent and Bubbly Systems, the DIERS research group has developed empirical correlations that relate the dimensionless superficial vapor velocity (B) at the point two-phase flow begins to the vessel vapor void fraction. The extent of disengagement, therefore, can be assessed by comparing the superficial velocity in the system (B_f) to the superficial velocity at the onset of two-phase flow (B). If the $B_f < B$, only vapor flow will occur. If $B_f > B$, two-phase flow will occur.

The Churn-Turbulent model is typically used for water-like fluids that do not foam and have low viscosity (<100 cP). The bubbles rise quickly while coalescing and dissociating in a random manner. For a cylindrical vessel, the dimensionless superficial vapor velocity at the onset of two-phase vapor-liquid flow can be determined by the empirical equation

$$\psi = \frac{j_{g\infty}}{U_\infty} = \frac{2\bar{\alpha}}{1 - C_o\bar{\alpha}}$$

where, ψ = the dimensionless vapor velocity at the onset of two-phase flow,

$J_{g\infty}$ = the superficial vapor velocity (ft/sec.), and

$\bar{\alpha}$ = the average vapor void fraction.

The term, C_o, is fit to experimental data and ranges from 1.0 (conservative) to 1.5 (best estimate). As a rule of thumb, all vapor venting will occur if the liquid inventory in the vessel drops below 33% of the vessel capacity (Becker et al 1998). Alternatively stated,

two-phase vapor-liquid flow will occur if the average vapor void fraction, $\overline{\alpha}$, is less than 67%.

The Viscous Bubbly model assumes uniform vapor generation throughout the liquid with limited bubble coalescing. Bubbles tend to keep their identity and to rise more slowly than in the Churn-Turbulent regime. This model is usually used for non-foamy, moderately viscous liquids (>100 cP). For the bubbly model

$$\psi = \frac{j_{g\infty}}{U_\infty} = \frac{\overline{\alpha}(1-\overline{\alpha})^2}{(1-\overline{\alpha}^3)(1-C_o\overline{\alpha})} .$$

The data correlation parameter, C_o, ranges from 1.0 to 1.5. The best estimate is usually given by C_o =1.2. The rule of thumb for Bubbly systems is that single-phase vapor venting will occur when $\overline{\alpha}$ > 83%.

CHAPTER 3

LABORATORY ANALYSIS OF DIKETENE DECOMPOSITION

3.1 Accelerated Rate Calorimeter Tests

A Columbia Scientific Accelerated Rate Calorimeter was used to characterize the decomposition of diketene. Six separate tests were performed using 1-2 ml of refined diketene (>98 wt%) in a 9.5 ml titanium sample bomb. The initial test conditions are shown in Table 3.1. The concentration of the reactants was measured by gas chromatography. No attempt was made to vary the concentration of acetic acid to determine the effect on initiation temperature. One of the six tests was conducted in a nitrogen atmosphere to determine if the reaction mechanism changed in a reduced oxygen environment.

The results of the ARC tests are summarized in Table 3.2 and Figures 3.1 and 3.2. The maximum observed self-heat rates in three of the six tests exceeded the upper limits of reliability of the ARC device (i.e. 15°C/min). These instantaneous maximum values are reported for completeness, but should not be used for analysis. At lower temperatures and pressures, the self-heat rate values are within the capability of the test and are therefore valid for analytical use.

TABLE 3.1: Initial Conditions for ARC Test

Sample ID	Diketene (wt%)	Acetic Acid (wt%)	Bomb Weight (g)	Sample Weight (g)	Weight Rem. After Test (g)	PHI	Initial Pres. (psia)	Initial Temp. (C)
80413	98.5	0.07	21.1373	1.0897	0.7967	4.88	14.1	25.4
80414	98.3	0.06	20.7813	1.0812	0.7950	4.84	14.1	27.8
80508-1*	98.0	0.00	21.0333	2.3455	1.7389	2.79	14.1	28.0
80518-1	98.1	0.07	21.2179	1.1788	0.8272	4.60	14.1	27.5
90127-1	>98%	N/A	21.7521	2.1927	1.3910	2.98	14.1	20.7
90203-2	>98%	N/A	21.1727	2.4722	2.4294	2.71	14.1	25.2

*Sample run in N2 atmosphere

TABLE 3.2: Summary Results from ARC Test

Sample ID	Onset Temp. (C)	Max. Pres (psia)	Temp. @ Max. Pres. (psia)	Observed Heat Rise (C)	Max. Self Heat Rate (C/min)	Max Press Rise (psi/min)	Final Pres. (psia)	Final Temp. (C)
80413	119.9	1899	253.8	103.5	6.4	181	616	35.8
80414	130.0	2309	293.8	111.8	46.0	2437	592	22.4
80508-1*	107.1	2319	441.5	182.0	337.5	4719	16	27.2
80518-1	92.1	630	286.1	128.6	2.3	18	212	36.4
90127-1	92.3	1254	302.3	210.6	408.6	3445	202	23.8
90203-2	101.3	**						

*Sample run in N2 atmosphere

**This sample was stopped when the self-heat rate =0.15 C/min in order to analyze the gases in the vapor space prior to complete conversion.

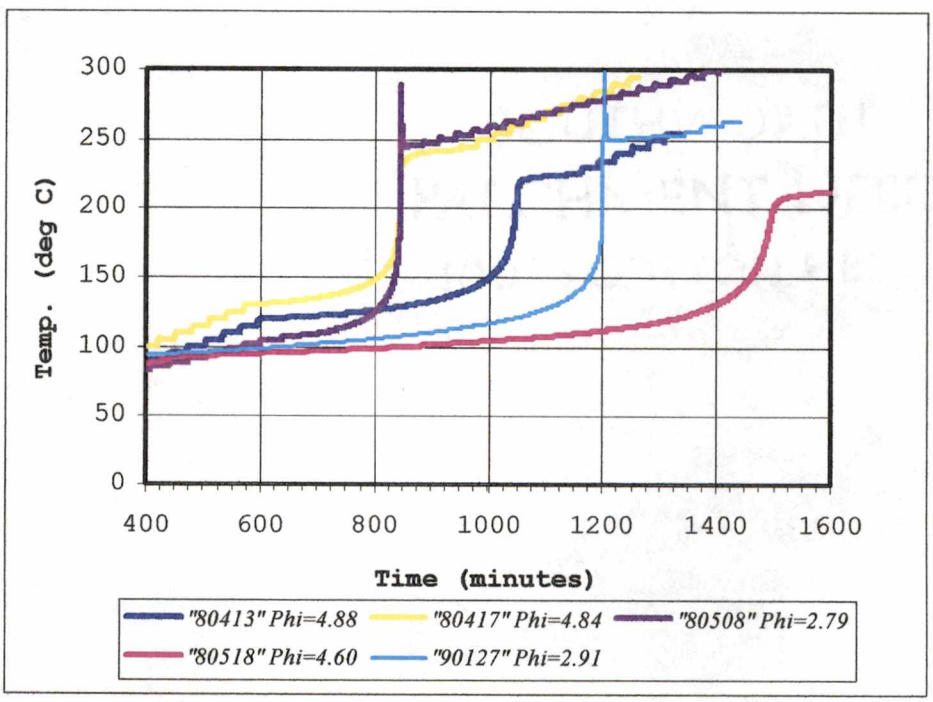

Figure 3.1: Measured Temperature Rise for Diketene Decomposition in ARC Device

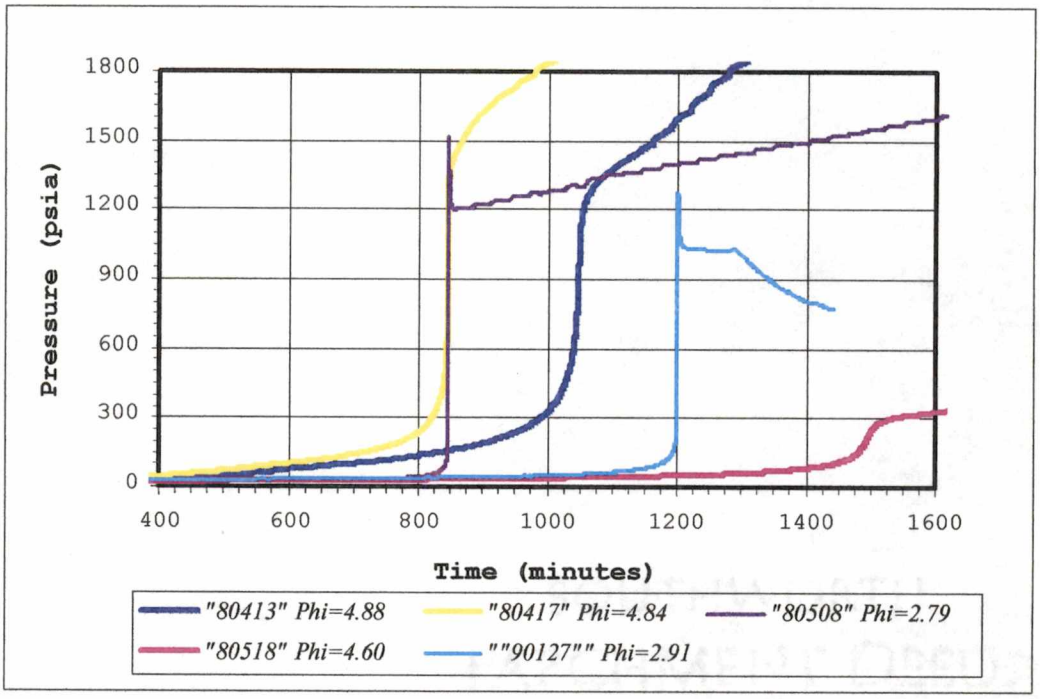

Figure 3.2: Measured Pressure Rise for Diketene Decomposition in ARC Device

The heat of reaction, adiabatic heat rise, and self-heat rates were calculated from the ARC data and are shown in Table 3.3.

There is significant and unexplained variability in the observed exotherm initiation temperature, self-heat rate, and the pressure rise. For the two tests with lower thermal inertia ($P < 2.8$), we would expect the pressure and temperature to increase much faster than in the tests in which $P > 4.6$. But this was not the case. Even after correcting for the thermal inertia (P) in the measured data, the variability is still significant. The reason for the variability remains unclear and does not appear to be attributable to the acetic acid concentration.

The reaction order and Arrhenius constants for the first sample were estimated by the ARC analysis software toolkit. The reaction order is 1.6. The activation energy is 30.71 kcal/gmol. The Arrhenius constant is 3.3×10^{13} sec^{-1}. As these estimates are provided from only one data point, they should be considered ballpark estimates.

The Log P versus $-1/T$ ($Kelvin^{-1}$) is plotted in Figure 3.3. From the non-linear behavior, we can easily conclude that the reaction behaves as a hybrid system producing both vapors and non-condensable gases. The question becomes then, what are the primary components of the gas stream and how many moles of non-condensable gases are being formed

TABLE 3.3: Calculated Values from ARC Data

Sample ID	Heat of Rxn (J/g)	Adiabatic Heat Rise (C)	Corrected Self-Heat Rate (C)
80413	1057	505.2	90.5
80414	1131	540.9	648.1
80508-1	1062	507.7	4758.0
80518-1	1237	591.6	31.8
90127-1	1313	627.6	5761.5
90203-2			
Avg Value	1160	554.6	2258.0
Std Dev.	112	54	2774

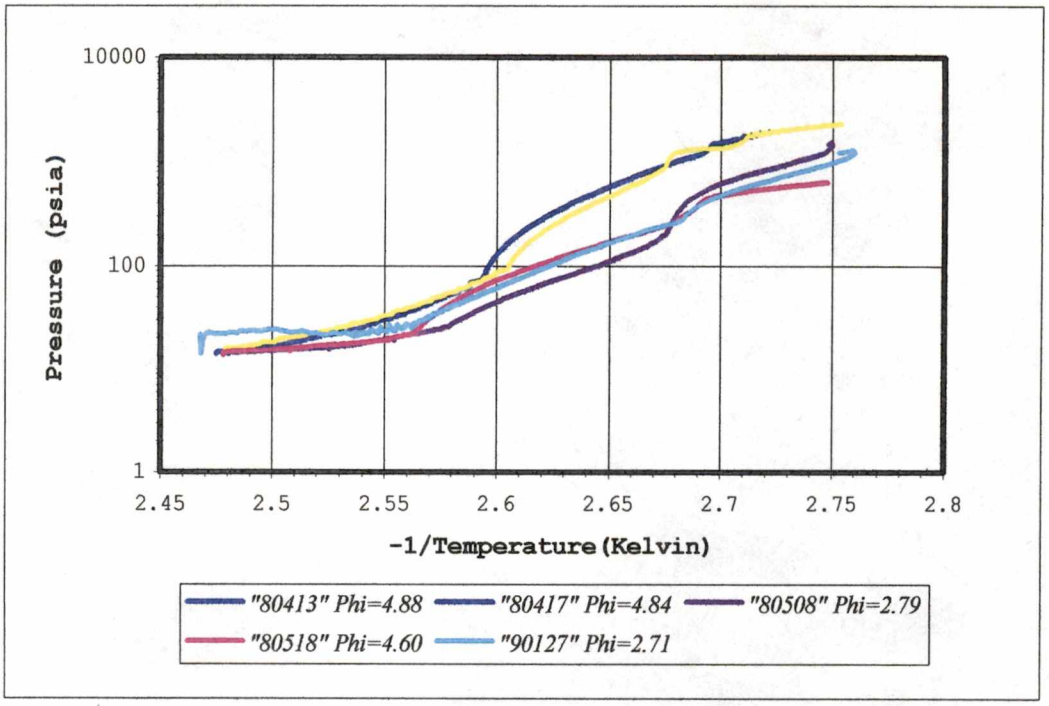

Figure 3.3: Log P versus Inverse Kelvin Temperature Data from Accelerated Rate Calorimeter Testing of Diketene

per mole of diketene consumed. The ARC data by itself is insufficient to provide this data without more knowledge regarding the reaction mechanism.

In an effort to obtain more information on the reaction mechanism, the last ARC test was stopped when the self-heat rate reached 0.15°C/min in order to analyze the intermediate compounds. Samples of the liquid and vapor space were collected from the bomb and analyzed by gas chromatography and mass spectroscopy.

The analysis of the gas sample proved to be inconclusive. Only air was detected. It is suspected that the sample bag was either insufficiently evacuated prior to sample collection or that there was a pinhole leak in the bag. On the other hand, the analysis of the liquid detected a strong presence of dehydroacetic acid (MW 168), 4-acetoxy-3-pente-2-one (MW 142), and dimethyl pyrone (MW 124) in order of abundance.

3.2 Bench-scale Distillation Tests

To further understand the diketene decomposition mechanism and to identify the volatile and non-volatile products, additional laboratory experimentation was conducted. Refined diketene was heated to 100°C for two hours in a stirred flask with overhead condenser unit. The overhead cooler condensed the vapors and refluxed these back to the flask. The condenser was vented to the laboratory hood to prevent pressure accumulation from non-condensable gases.

The composition of the initial liquid charge was analyzed by GC mass spec. After two hours at 100°C, the liquid was again sampled and analyzed by GC mass spec. The diketene was cooled and stored at room temperature in an open container for 8 days. After the 8 days, GC mass spec was again used to analyze the diketene liquid. On the eighth day, the liquid diketene was reheated to 100°C and analyzed once again by GC Mass spec. The GC Mass Spec analysis of the diketene tars is shown in Table 3.4. Not all components detected are represented in the table. Acetic acid, ethyl and methyl acetate, benzene, toluene, and trace amounts of other components were detected. However, the rate of change of these compounds was small compared to the compounds listed in Table 3.4

From the results of the GC Mass spec, the initial liquid consisted primarily of diketene, acetic anhydride, methyl diketene, and acetone in order of relative abundance. After the first 2-hour heat cycle, the methyl diketene concentration increased by 38% and the acetone concentration increased by 69%. Dehydroacetic acid (DHA) was also observed in significant abundance after the 2-hour heat cycle.

Over the next 8 days, the acetone and DHA concentration more than doubled while the methyl diketene only increased by 28%. Small amounts of dimethyl pyrone and 4-acetonxy-3-pente-2-one (C7H10O3) were also noted in the sample. Following the final heat cycle, there was a

dramatic increase in the abundance of DHA and dimethyl pyrone. The DHA concentration tripled and the pyrone concentration increased more than seven fold. The acetone, methyl diketene, and C7H10O3 showed only modest increases.

The GC mass spec results from the distillation experiment were compared to previous analyses of diketene tar samples from other (non-related) experiments. The results were surprisingly comparable to the bench-scale distillation. The previous work indicated the presence of the same compounds identified in Table 3.4. In addition, compounds with higher molecular weights were also noted such as 192, 208, 210, 234, 252, 254, 276, and 294. The conditions under which the previous work was performed were unknown to this author. But it is suspected that these tars were formed from diketene that was exposed to either higher temperatures or longer heat cycles.

3.3 Analysis of Diketene Decomposition Mechanism

From the technical research and the experimental data, it is clear that diketene dimerizes to form dehydroacetic acid (DHA) and continues to polymerize to form other higher molecular weight compounds. The molecular weights of the polymeric compounds correspond to even

TABLE 3.4: GC Mass Spec Analysis of Diketene Tars

Compound	Mol. Wt.	Relative Abundance			
		Before heating	After 2 hr heat	After 8 day storage	After Reheat
Acetone	58	68000	116000	226000	380000
Methyl Dk	98	124000	160000	230000	260000
Dimeth Pyrone	124	0	0	22000	140000
4-acetoxy-3-pente-2-one	142	0	18000	82000	170000
DHA	168	0	90000	208000	640000
unkn.	208	0	0	16000	60000
unkn.	210	0	0	16000	40000

multiples of ketene (MW 42) corresponding to the degree of polymerization. For example, polymeric compounds with molecular weights of 210 and 252 were observed. The degrees of polymerizations are thus 5 and 6, respectively (e.g. 5 x 42 = 210).

The polymerization mechanism alone does not explain the formation of non-condensable gases. The results of the bench scale distillation suggest that a condensation mechanism in which non-condensables are generated occurs in parallel with polymerization mechanism. From the molecular weights, the non-condensable gas appears to be carbon dioxide (MW 44). The data also suggest that water (MW 18) is being formed and consumed during the course of the reactions.

From the analysis of the molecular weights, two parallel reaction mechanisms are proposed (see Figure 3.4). The heated diketene first begins to polymerize. As the temperature increases, the large polymer molecules begin to cleave water. The majority of the water formed is assumed to react with diketene to form acetone and CO_2. However, trace amounts of water are sufficient to catalyze the DHA (MW 168) to dimethyl pyrone (MW 124).

As the temperatures approach the boiling point of diketene, the heat hastens the dehydration of the large polymer molecules. At these higher temperatures, the water then reacts very rapidly with the diketene to form carbon dioxide and acetone. The hydrolysis reaction liberates more energy, which in turn raises the temperature and cleaves more water from the polymer molecules. This cycle begins to accelerate until diketene is completely consumed. Thus, the dehydration is assumed to be the rate-limiting step.

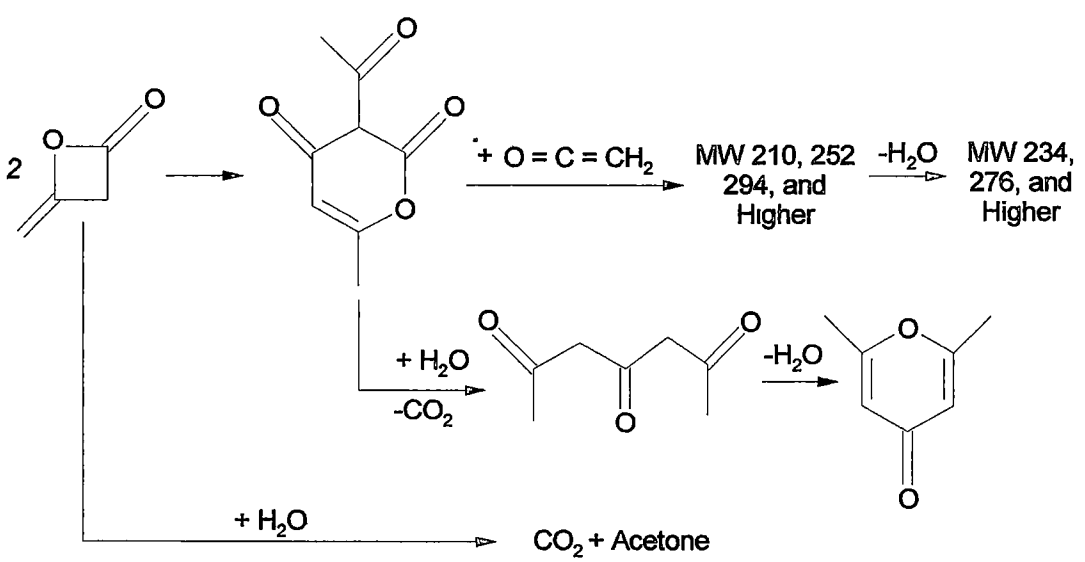

Figure 3.4: Proposed Decomposition Method for Diketene

CHAPTER 4

DEVELOPMENT AND EVALUATION OF DECOMPOSITION MODEL USING DYNAMIC SIMULATION

4.1 Development of Reaction Models

The bench-scale distillation testing was conducted concurrently with the development of the dynamic model. However, the results of the bench-scale distillation were not available until after the completion of the dynamic modeling. Consequently, the simulation model that was used does not exactly agree with the proposed decomposition method. Despite this, the "assumed" reaction mechanism used in the computer model predicts the temperature, pressure, and energy behavior in the system very well and is suitable to predict operating conditions which will prevent the runaway scenario.

This approach demonstrates that in the absence of well-defined reaction mechanisms, simple assumptions can be used to develop suitable dynamic models to simulate the physical process. In many well-behaved reaction systems (i.e. those that follow simple Power Law behavior), expensive laboratory tests to fully understand the reaction mechanism may be averted.

The first step in developing the reaction model is to determine how many moles of non-condensable gas are being formed. The answer lies in the clues from the ARC data and a basic knowledge of acetyl chemistry. Theoretically, after the ARC bomb has been cooled, the residual pressure results from the presence of volatile and non-condensable components. We can assume, however, that all of the volatile components have condensed and that the pressure is solely a function of the non-condensable gases. This is a reasonable assumption if the residual pressure is very high when compared to the vapor pressures of the suspected volatile products. In this case,

acetone is the lightest volatile component expected to be present. The vapor pressure of acetone at 36°C is less than 7 psi. Yet in the first ARC test, the residual pressure is 602 psi (616.1 psia - 14.1 psia, see Table 3.1). Therefore, assumption of all non-condensable gas imposes little error.

Furthermore, we assume that the non-condensable gas is CO_2. This too is a reasonable assumption since CO_2 is a known gas by-product of many high temperature reactions involving acetyl compounds. We can calculate the gas generation rate from the loss of mass during the experiment. For example, in the first ARC test, the mass lost is 0.293 g. The number of moles of gas generated per mole of diketene is thus 0.52 (=0.985 × 0.293 g / 44 g per gmol CO_2). The average value for the six runs is 0.53 moles of gas generated per mole of diketene (refer to Table 4.1). This is close to the gas generation rates reported by Fuller (1984).

The next step is to formulate possible reactions and simulate these models under the conditions of the ARC test. Simply stated, we guess the reaction mechanism, insert it into a computer simulation of the ARC bomb, them compare the temperature and pressure rise to the ARC results. This allows us to determine if the proposed reaction

Table 4.1: Estimated Number of Moles of Carbon Dioxide Generated by Decomposition of Diketene

Sample ID	Est. CO2 Generation (mol/mol Dk)
80413	0.521
80414	0.514
80508-1*	0.504
80518-1	0.581
90127-1	N/A
90203-2	N/A
Avg Value	0.530
Std Dev.	0.034

mechanism is suitable to use for simulating the behavior of diketene in the actual chemical process.

Because of the uncertainties in this approach, four separate models are evaluated as shown in of Figure 4.1. The first reaction is based upon the published reaction in which one mole of dimethyl pyrone and one mole of CO_2 is formed per every two moles of diketene consumed. The second proposed reaction is a purely hypothetical reaction in which two moles of non-condensable gas and two moles of non-volatile sludge (i.e. carbon) are formed per mole of diketene reacted. This second reaction was proposed because of the assumption that it will conservatively estimate the pressure changes. The third reaction is also a hypothetical reaction with condensable, non-condensable, and non-volatile products.

The third reaction neglects that water and diketene are highly reactive. Therefore, the fourth proposed reaction is virtually identical to the third reaction, except diketene is hydrolyzed by water in a parallel reaction.

The simulation results are evaluated in Section 4.2. Because of the wide variation in laboratory results, the criterion for selection is not necessarily the best fit for the data. Instead, the best model in this case is more conservative than the laboratory data. Ultimately, the model that is selected conservatively predicts the rate of both temperature and pressure increase.

4.2 Validation of Reaction Model Using Dynamic Simulation

The computer simulation of the Accelerated Rate Calorimeter consists of a 9.5 ml flash tank containing approximately 1 ml of diketene (98.5 wt%). As the reaction proceeds, the material in the flash tank transfers heat to the shell, which is modeled as a pseudo-liquid system having physical properties (i.e. density and heat capacity)

Proposed Reaction Model #1:

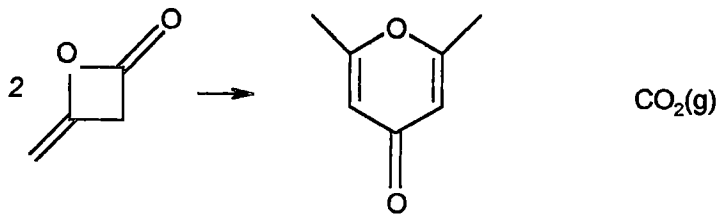

Proposed Reaction Model #2:

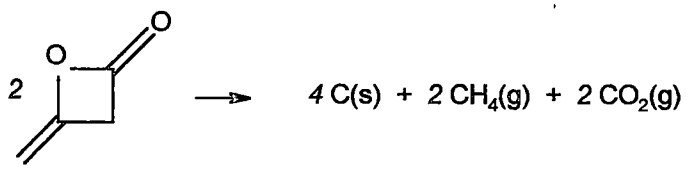

Proposed Reaction Model #3:

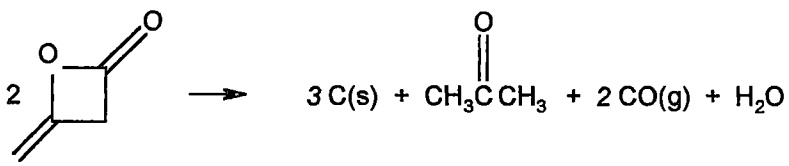

Proposed Reaction Model #4:

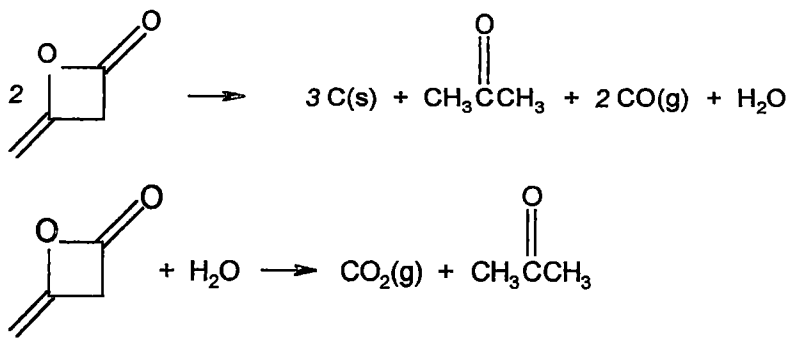

Figure 4.1: Proposed Reaction Models for Diketene Decomposition

corresponding to titanium. A conceptual representation of the computer simulation for the ARC test is shown in Figure 4.2.

Each of the proposed reaction mechanisms is simulated and the pressure and temperature rise compared to ARC results. The physical property and vapor-liquid equilibrium (VLE) data sets used to model the system is shown in Appendix A. The simulation is designed such that the phi corresponds to the highest phi factor of the six ARC runs (P = 4.88). For the three ARC runs with high phi factors (4.60-4.88), the self-heat rate remained, for the most part, within the measurement limits of the ARC device. Therefore, these three runs serve as the basis for comparison to the simulation results.

The reaction rate used for all four proposed reaction mechanisms is a simple first order Power Law model

$$\frac{dC}{dt} = K_{for}C \text{ , where}$$

Reaction Rate: units of dC/dt = lbmol/(hr ft^3)

Units of C = lbmol/ft^3

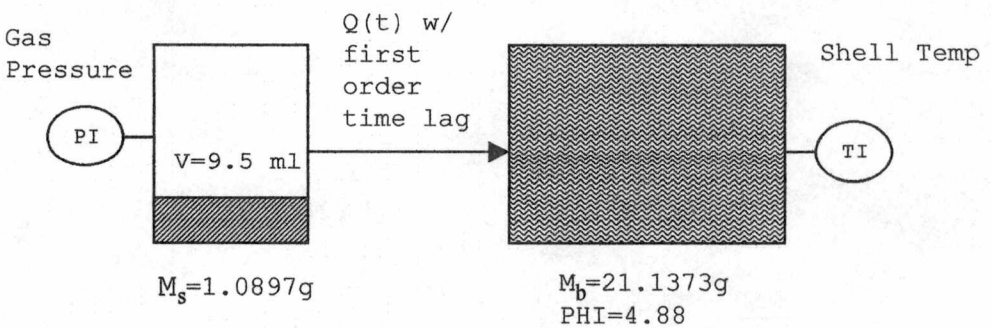

Figure 4.2: Conceptual Representation of Computer Simulation of ARC Test.

Rate Constants:	$K_{for} = A * e^{(-E/RT)}$
	A = Arrhenius constant, (1/hr)
	E = Activation energy, (cal/gmol)
	[R = 1.987 cal/(gmol K), T in Kelvin]
Heat of Reaction:	42,000 BTU/lbmol Diketene consumed.

Although the ARC test provides preliminary estimates of the A and E, the first simulations revealed that these estimated values were not suitable. Several iterations of A and E had to be tried to find more suitable values. The A and E terms are not mutually exclusive and cannot, therefore, be manipulated completely independently. But in general, lower activation energies result in lower onset temperatures. Increased values of the Arrhenius constant increase the self-heat rate. Therefore in the simulation, A and E were varied according to Figure 4.3 to determine the best fit for the constants.

For the proposed reaction mechanism #1, the simulated temperature rise and the ARC results are compared in Figure 4.4. The simulation results are labeled B3, B4, C4, etc. corresponding to the choice of activation energy (E) and the Arrhenius constant (A) as shown in Figure 4.3. The simulation and the ARC temperatures match reasonably well using a low value for E and a mid-range value for A.

On the other hand, the simulated pressure rise for the proposed mechanism #1 does not match the ARC results (see Figure 4.5 on page 40). In all cases, the reaction model fails to reach the maximum pressure observed in the ARC test. The reason is that the pressure is primarily a function of the moles of CO_2. The dimethyl pyrone imparts almost negligible vapor pressure and the only volatile component, i.e. diketene, is being consumed by the reaction. Consequently, the proposed reaction mechanism #1 is a poor choice for modeling diketene behavior in the real chemical process.

For the proposed reaction mechanism #2, the simulated temperature and pressure rise are compared to the ARC results (see Figures 4.6 and

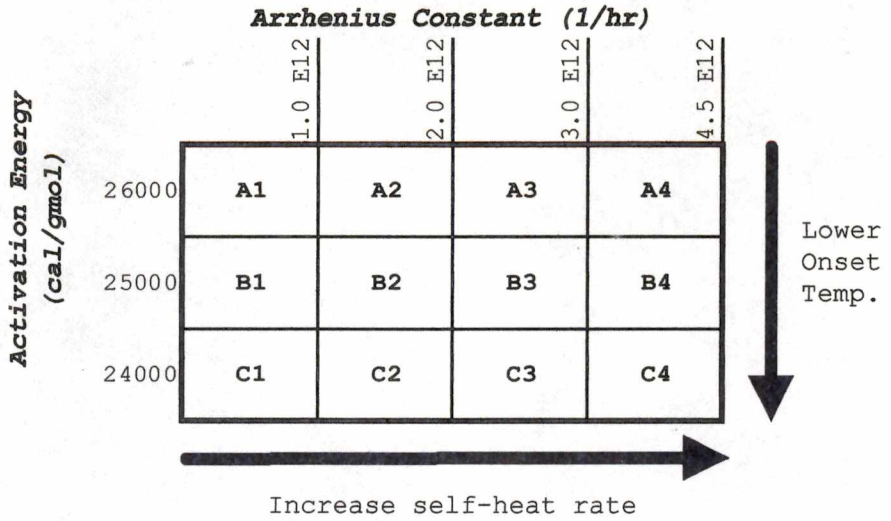

Figure 4.3: **Key Plan Indicating the Effect of Varying the Arrhenius Constant and Activation Energy in Dynamic Simulation of the Runaway Reaction of Diketene.**

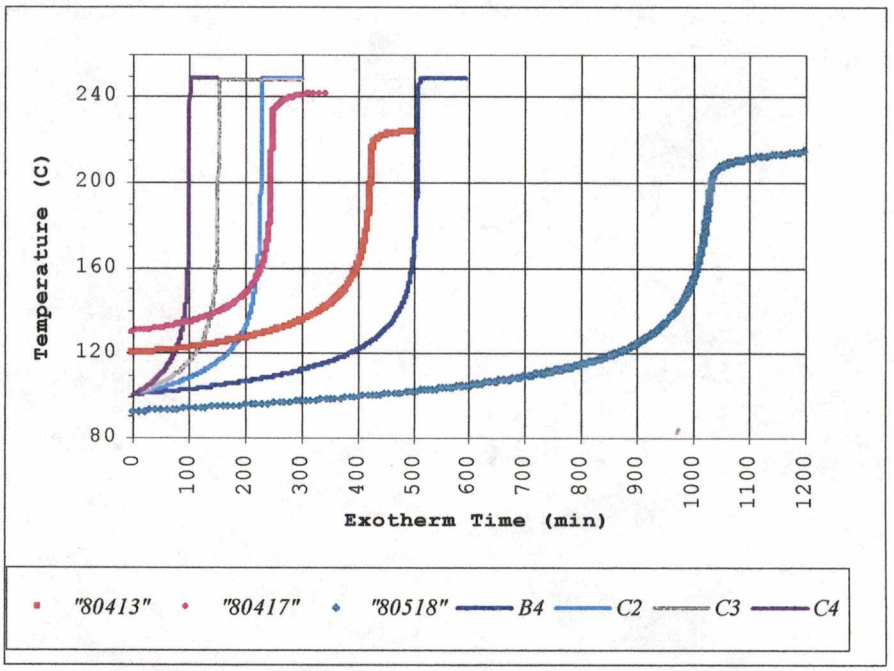

Figure 4.4: **ARC Temperature Results Compared to Computer Simulation Using Proposed Reaction Mechanism #1 and Varying Activation Energy and Arrhenius Constants.**

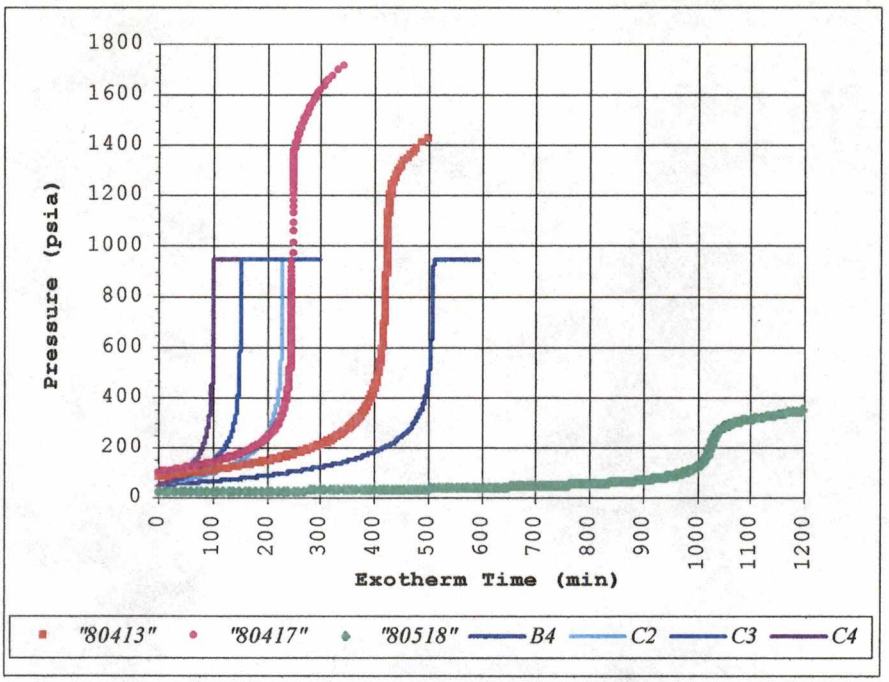

Figure 4.5: ARC Pressure Results Compared to Computer Simulation Using Proposed Reaction Mechanism #1 and Varying Activation Energy and Arrhenius Constants.

4.7 on page 41). For this reaction, the simulated pressure agrees well with the ARC data in all cases. But the simulated temperature rise does not. Furthermore, the self-heat rates are much lower for the proposed mechanism #2 than are observed in the ARC test (see Figure 4.8 on page 42). Even with low values of E and high values of A, the rates of temperature and pressure increase are not fast enough. Consequently, this mechanism is not sufficiently conservative and is therefore not suitable for the plant-scale model.

For the proposed reaction mechanism #3, the simulated pressure, temperature, and self-heat rates are compared to the ARC results in Figures 4.9-4.11 on pages 42 and 43. The model agrees well with the observed temperature, pressure, and self-heat rates. The simulation "C3" shows that the Arrhenius constant ($A=2.0 \times 10^{12}$ hr^{-1}) and activation energy (E=24000 cal/gmol) are sufficiently conservative for modeling the runaway behavior of diketene.

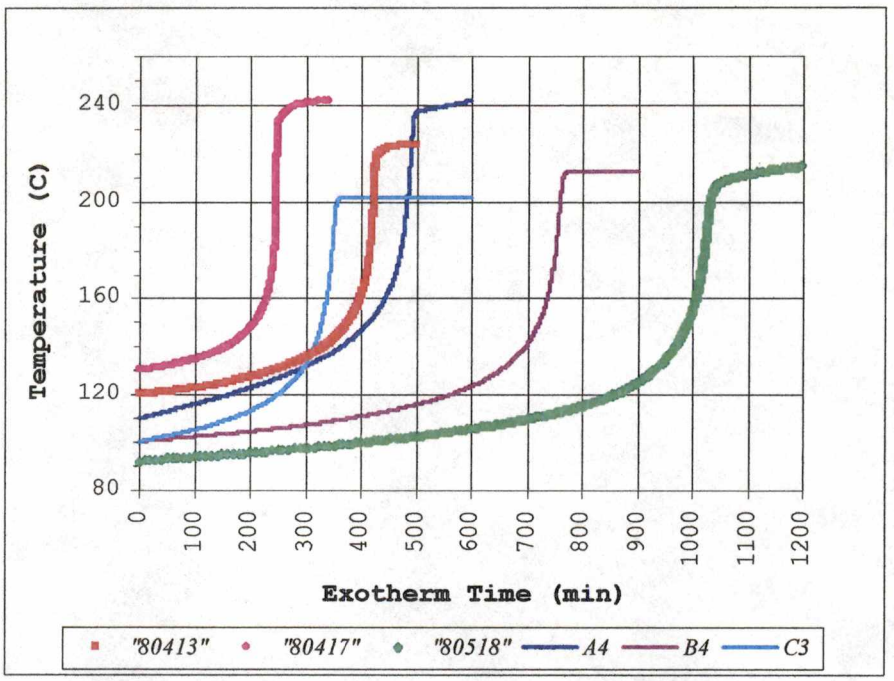

Figure 4.6: ARC Temperature Results Compared to Computer Simulation Using Proposed Reaction Mechanism #2 and Varying Activation Energy and Arrhenius Constants.

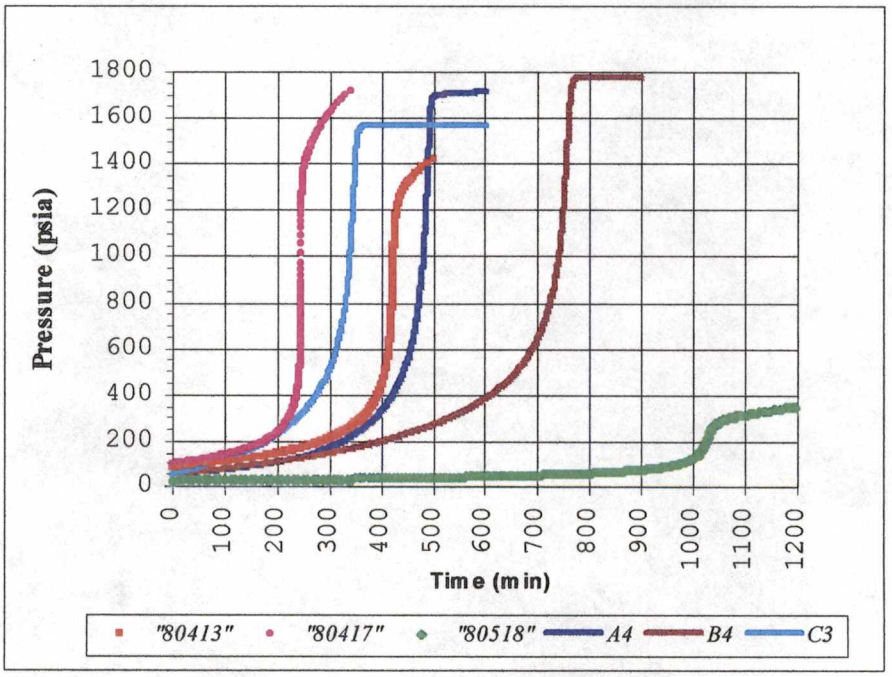

Figure 4.7: ARC Pressure Results Compared to Computer Simulation Using Proposed Reaction Mechanism #2 and Varying Activation Energy and Arrhenius Constants.

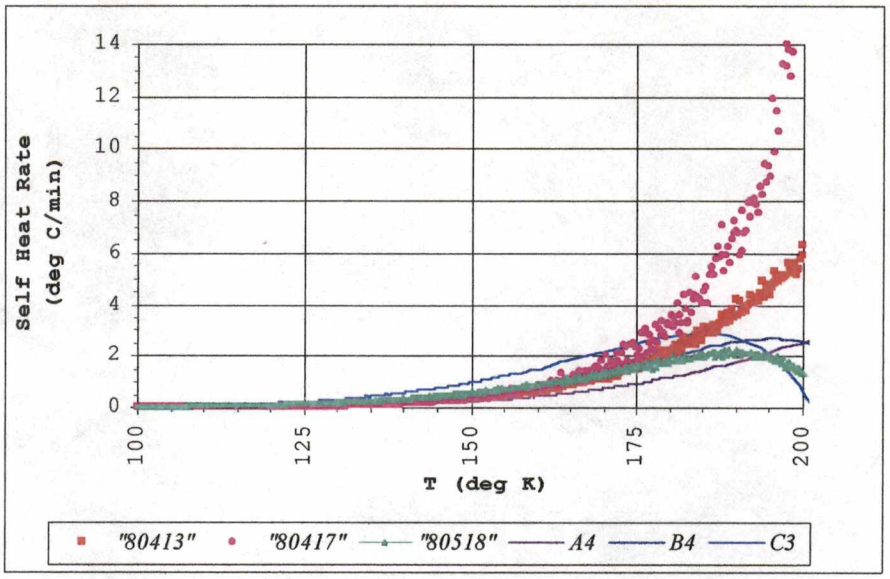

Figure 4.8: **ARC Self-Heat Rates Compared to Computer Simulation Using Proposed Reaction Mechanism #2.**

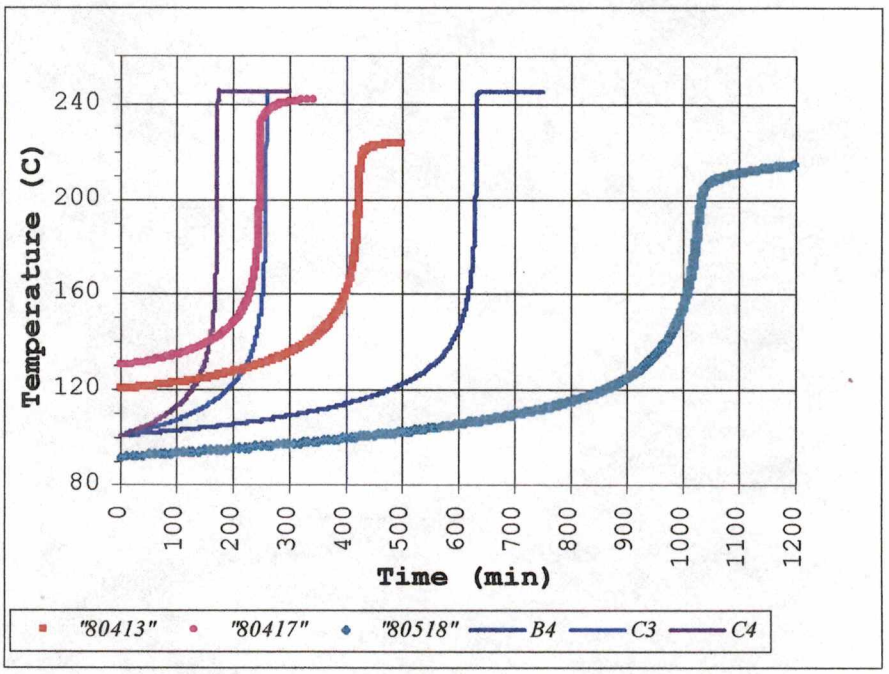

Figure 4.9: **ARC Temperature Results Compared to Computer Simulation Using Proposed Reaction Mechanism #3 and Varying Activation Energy and Arrhenius Constants.**

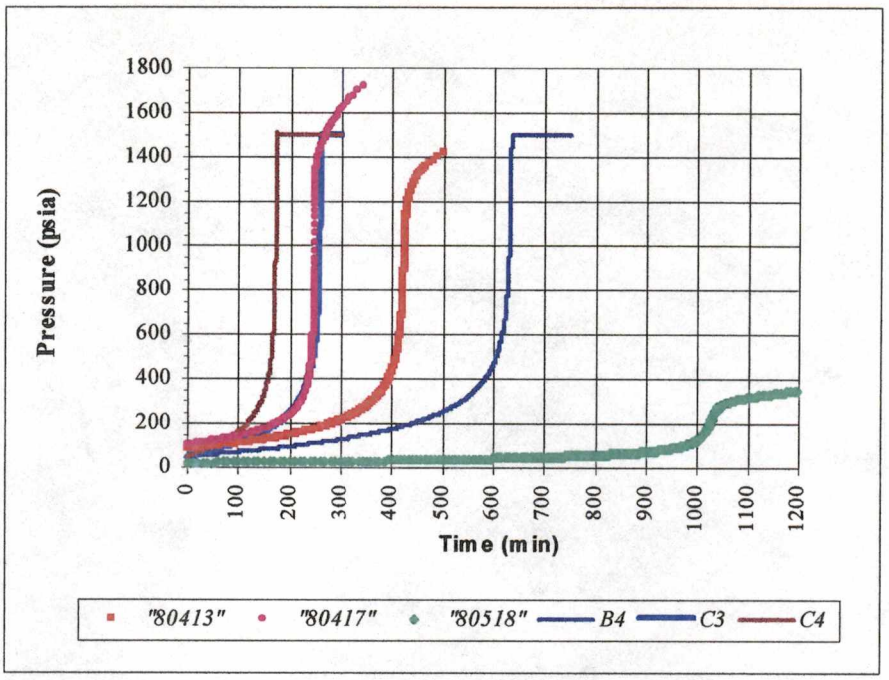

Figure 4.10: **ARC Pressure Results Compared to Computer Simulation Using Proposed Reaction Mechanism #3 and Varying Activation Energy and Arrhenius Constants.**

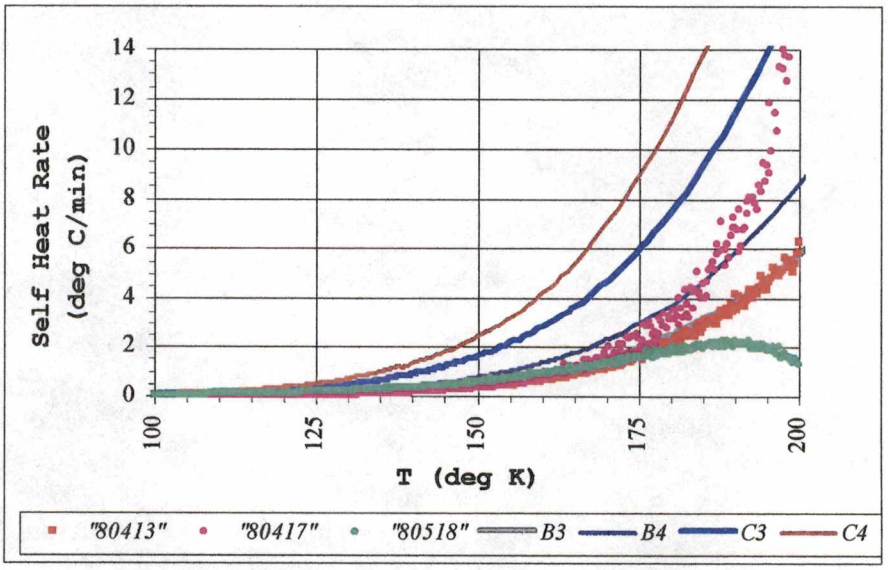

Figure 4.11: **ARC Self-Heat Rates Compared to Computer Simulation Using Proposed Reaction Mechanism #3.**

The proposed reaction mechanism #4 is identical to mechanism #3, except for the addition of a parallel reaction of diketene and water. Although the proposed mechanism #3 seems to agree well with the ARC data, there is a caveat in using a reaction mechanism that would allow for accumulation of water in a predominantly organic system. The concern is a problem with the heat balance when water is present. The heat of vaporization of water (~950 Btu/lbm) is nearly 4 times that of diketene (~200 Btu/lbm). In a closed system when no vapors are being removed from the system, the accumulation of water does not significantly affect the heat balance of the system. However, in an open or "vented" model, water will vaporize before diketene. Consequently, the simulation may predict more heat lost by vaporization than will actually occur. Thus, the parallel hydrolysis reaction is suggested for reaction #4 to ensure water accumulation does not occur. The rate-limiting step is assumed to be the formation of water. The hydrolysis reaction happens instantaneously.

The simulated pressure, temperature, and self-heat rates for the proposed reaction mechanism #4 are compared to the ARC results in Figures 4.12-4.14. The model predictions for the temperature, pressure, and self-heat rates are much more conservative than are observed in the ARC. The model also proves to be least sensitive to variations in the activation energy (E) and Arrhenius constant (A). For these reasons, the proposed mechanism #4 appears to be a suitable choice to use in simulating the full-scale plant system.

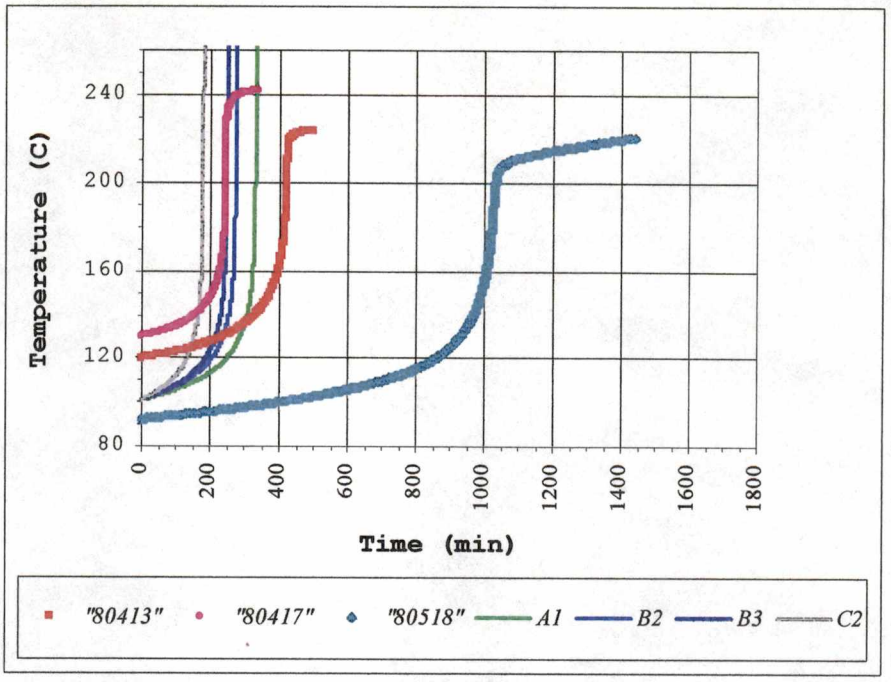

Figure 4.12: ARC Temperature Results Compared to Computer Simulation Using Proposed Reaction Mechanism #4 and Varying Activation Energy and Arrhenius Constants.

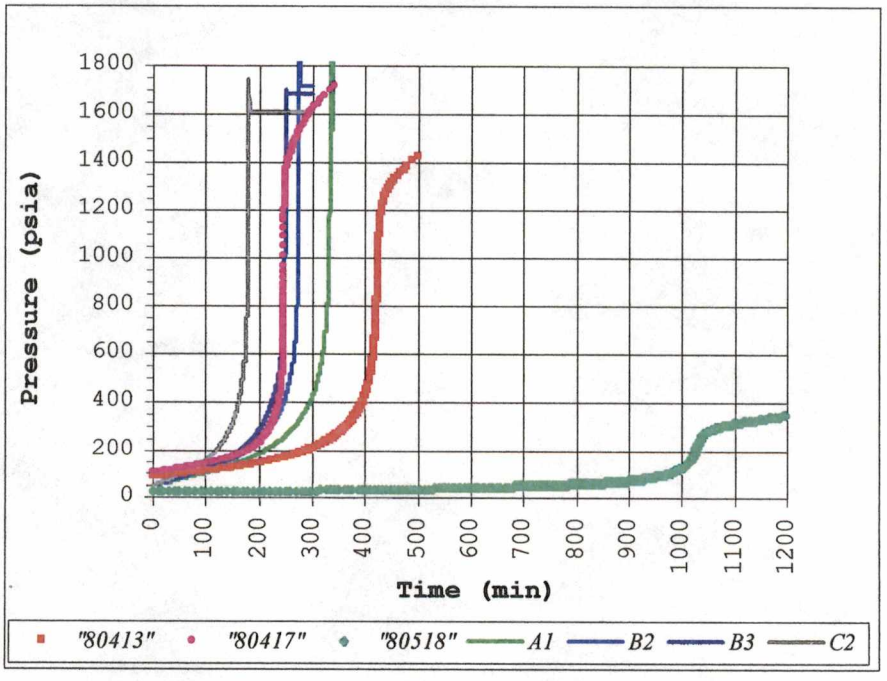

Figure 4.13: ARC Pressure Results Compared to Computer Simulation Using Proposed Reaction Mechanism #4 and Varying Activation Energy and Arrhenius Constants.

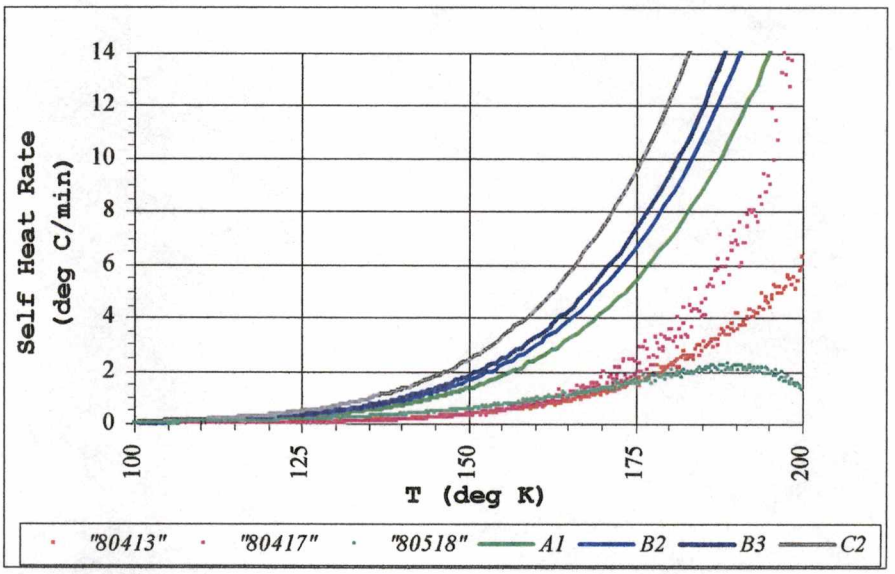

Figure 4.14: **ARC Self-Heat Rates Compared to Computer Simulation Using Proposed Reaction Mechanism #4.**

CHAPTER 5

EVALUATION OF REFINING COLUMN SAFETY SYSTEMS USING DYNAMIC SIMULATION

5.1 Process Description

As previously noted, diketene is manufactured by the pyrolysis of acetic acid. A typical diketene production facility is illustrated in Chapter 11 of Agreda and Zoeller's text (1993). When diketene is manufactured in this manner, acetic anhydride and other high boiling impurities are formed in portions of 8 to 10 percent of the crude diketene (Bergmin et al 1991). Trace amounts of light components are also present such as acetic acid and acetone. The refining step is used to segregate the pure diketene from the light and heavy byproducts. Because of the simplicity of the refining process and because of the relatively pure state of diketene obtained therefrom, this refining step has been chosen to demonstrate the power of dynamic simulation and calorimetric testing in developing process safety systems that prevent runaway reactions.

The refining process is shown in Figure 5.1. An initial flash evaporation step is used to remove most of the high boiling impurities. The crude diketene is heated and vaporized under reduced pressure conditions. A vapor-liquid separator pot removes the non-volatile sludge and polymeric solids in the underflow. The vapor overflow from the separator pot is predominantly diketene and acetic anhydride but contains some very low boiling impurities. The vapor stream is cooled and condensed under reduced pressure whereby the very light components exit via the vacuum system. The distillation column, therefore, primarily separates diketene from the anhydride.

The column operates also under vacuum to further remove any light components and to ensure the processing temperatures do not exceed the

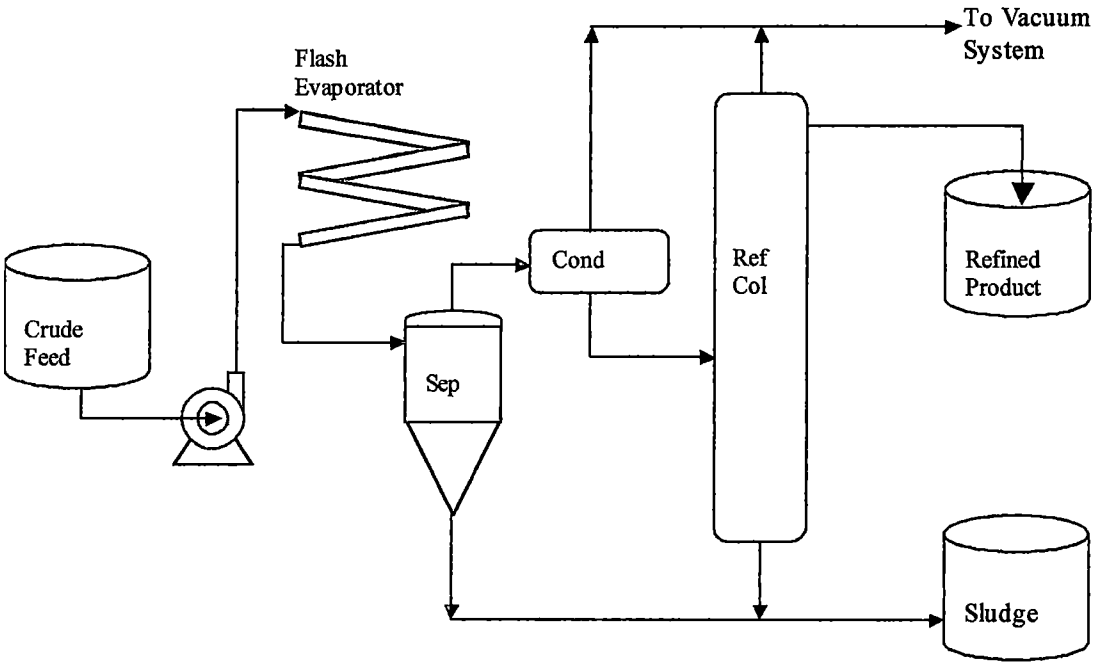

Figure 5.1: Refining Process for Crude Diketene.

self-accelerating decomposition temperature (SADT) of diketene. The column reboiler and overhead condenser are not shown. The refined diketene exists in the distillate and is cooled (cooler not shown) and collected in a temperature-controlled product tank. The bottom stream, which contains anhydride and other high boiling impurities, is pumped (pump not shown) to a temperature-controlled sludge tank.

5.2 Simple Computer Model of Refining Column

It is theoretically possible to model the refining column as a reactive distillation column. In such a model, the reaction is assumed to occur as a function of the composition, temperature, and liquid holdup on each stage. In practice, however, stage-wise modeling of a runaway reaction can cause several problems with convergence routines and significantly slow the processing speed. The reactions occur so quickly and liberate so much heat, that the liquid inventories per stage quickly dissipate to zero as the total number of

molecules vaporize. The incremental time steps for the mathematical calculations must be very small, on order of hundredths of a second. Furthermore, the overall pressure rise during the runaway reaction is substantially greater than the stage-to-stage pressure changes under normal operations. Unless there is good reason, such as large inventories per stage or intermediate reboilers, simplified models are preferentially used for modeling runaway systems.

For this case, the refining system is modeled as a series of flash tanks (see Figure 5.2). The column itself is represented by two independent flash tanks to allow independent manipulation of the reboiler and condenser duties (Q_r and Q_c, respectively). As a conservative approach, the volume of the first flash tank represents only that portion of the column in the base and reboiler (i.e. the volume below the bottom tray or packed section). Yet, the liquid inventory represents the entire holdup in the column (i.e. includes the base, the reboiler, and the holdup on each tray or the wetted surface of the packing).

The second flash tank represents the overhead condenser and reflux (see Figure 5.2). The volume and inventories of vapor and liquid match the process conditions in the condenser and reflux pot.

The operating conditions for the process illustrated by Agreda and Zoeller (1993) are not reported. Therefore, the base conditions for modeling of the refining column (see Appendix A) are somewhat arbitrary and are intended to exemplify a typical diketene refining process and not a specific one. With the pressure drop across the trays or packed section modeled as vapor flow through an orifice, the top pressure was varied until the temperature in the bottom of the column was at or below the SADT of diketene. The reboiler and condenser duties are determined by the reflux ratio (L/D). By using this simple model, the mass and energy terms (Q_1, Q_2, Q_R, and Q_C) can be manipulated independently to determine their effect on the process. Several assumptions are used in building the computer model,

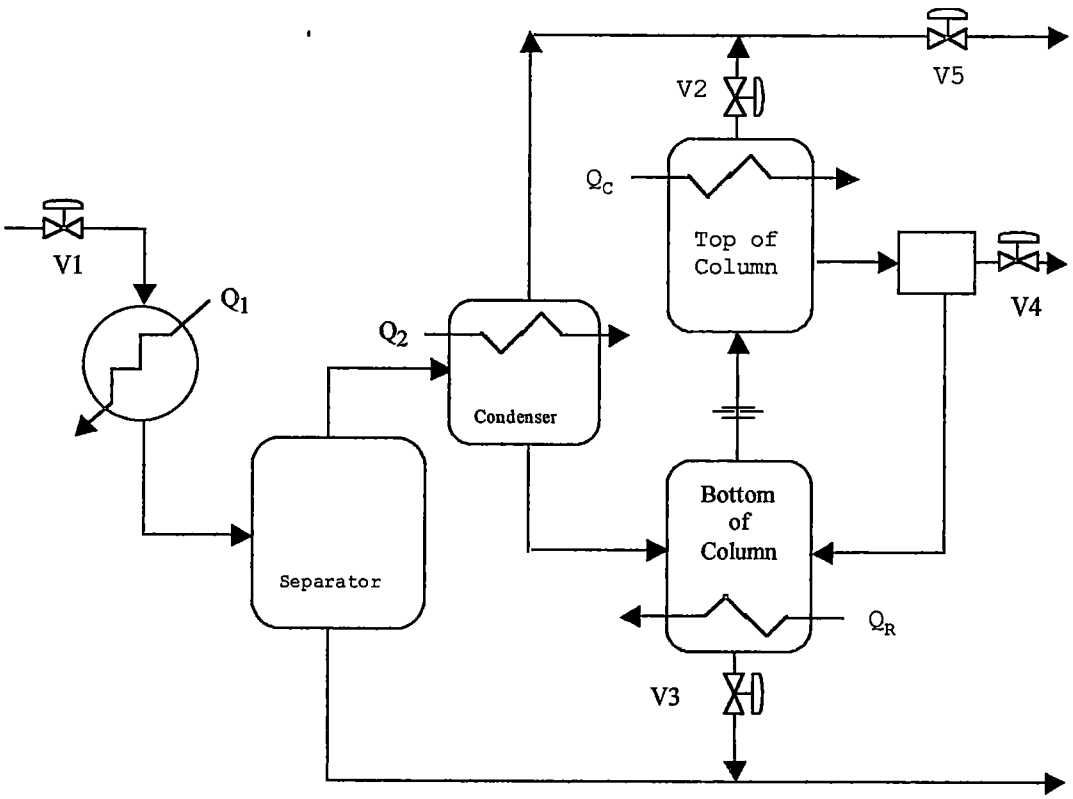

Figure 5.2: **Conceptual Representation of Computer Model for Refining Column.**

which are intended to provide very conservative predictions of the temperature and pressure behavior. The heat lost through the insulated vessel walls is neglected. Perfect mixing is assumed in both the liquid and vapor phases. The total "void" volume in the model represents only a portion of the total void volume in the physical process. The vapor volume between the bottom tray (or bottom of packing) and the top tray or bed limiter is neglected. The pressure drop across the packing is modeled as a constant-area restricting orifice. Thus as the vapor flow increases in the column, the pressure drop increases with the squared value of the flow rate until choked flow conditions are reached.

The model also includes several constraints where such constraints may exist in the physical process. For example, the condenser duty is limited to 110% of the base set condenser duty. On the other hand, the maximum allowable external heat source is limited to five times the normal reboiler duty. This would represent either a severe design case or a possible fire. The vacuum system is also limited to 110% of the base case vapor loading in cubic feet per minute.

The dynamic simulation computer program is a robust tool for evaluating the potential diketene runaway reaction. Unfortunately, the simulation package does not have the capability to model two-phase vapor liquid flow. Consequently, the process model is limited to the range of operation in which vapor and liquid completely disengage and all-vapor venting occurs. The maximum pressures the model can simulate accurately correspond to a pressure rise of 1650 Torr in the base of the column. This coincides with the assumed set pressure of a hypothetical relief device in the base of the column.

5.3 Emergency Shutdown System

Most distillation column control strategies include computer logic to stop the column operation upon detection of any abnormal increase in temperature or pressure. This is a critical safety component when the

potential for a runaway reaction is present. The intent of the control strategy is to detect the conditions that may lead to a runaway reaction of diketene and shutdown the column operation before the runaway can occur. A typical automated emergency shutdown (ESD) program for a highly reactive chemical such as this would monitor the temperature in bottom of the column, the pressure in the top, and the cooling water flow. If high pressure, high temperature, or low flow is detected, the emergency shutdown system would execute the following sequence (refer to Figure 5.2 for valve labels, etc.):

(a) Close the main feed valve (V1) to the refining system,
(b) Stop the steam flow to the reboiler (Q_R=0) by closing two automated steam valves in the steam supply,
(c) Open a condensate drain valve on the reboiler to quickly remove hot condensate from the reboiler,
(d) Close the column underflow valve (V3),
(e) Close the column take-off valve (V4), and
(f) Open the vapor valve to the vacuum system (V5).

In addition to the actions listed above, the control system might also operate a dump, quench or inhibitor dosing system. A dump system will rapidly drain the vessel inventory by opening a special drain valve. Quench systems act to cool the column contents by means of direct contact cooling. Inhibitor dosing systems usually rely upon another chemical to terminate the runaway reaction by altering the reaction mechanism. These alternate safety options pose special problems and require special precautions. These alternatives should be fully explored before implementation. Dynamic simulation is a powerful tool that can be used to assess the performance of the emergency shutdown system as well as explore the benefit of these additional safety options.

For diketene, there are few commercially available tried-and-true inhibitor-dosing agents. Most of the known inhibitors are metal or nonmetal halides or acid chlorides. Elementary sulfur and sulfur

dioxide have shown some success in reducing the formation of polymeric compounds (Bergmin et al 1991). But none of these agents have been touted as capable of inhibiting a vigorous decomposition of diketene.

Dump systems, especially for diketene, pose significant hazards. To avoid the strong vapors, diketene should be dumped either into another vessel or subsurface into another compatible liquid. Whichever option requires some means to safely vent the CO_2. Although highly reactive with water, diketene can be dumped into a water bath provided there is a very large excess of water to ensure dilution and the safe dissipation of heat. The polymeric byproducts normally present in diketene also pose a difficult problem for the dump valves. The polymer solids accumulate in the normally closed dump valves and may prevent the dump valves from operating properly if needed.

Quench systems also have problems, most notably the availability of suitable quench agents. Acetic anhydride, acetic acid, toluene, xylene, and butylacetate are suitable quenching agents for diketene.

5.4 Evaluation of Failure Modes

The advantage of using a computer model for a process containing a potential runaway reaction is that we can evaluate various emergency response strategies under extreme conditions that may be too dangerous to attempt in a real process. To demonstrate this, the dynamic simulation of the diketene refining process is subjected to three independent failures i.e.

A. loss of the condenser cooling (Q_c=0),
B. loss of the vacuum system, and,
C. maximum heat input ($Q_{r,max}$= 5 x Q_r).

For each failure scenario, the emergency shutdown system is activated and the temperature and pressure are observed. For example, the first simulation demonstrates the performance of the emergency shutdown

(ESD) system when the column looses water to the condenser. Additional simulations are then run using a quench system or dump system along with the ESD system. The initiation temperature for the ESD is assumed to be 40°C above the normal base temperature. In the last simulations, failures are repeated but the ESD initiation or "trip" temperature is lowered by 20°C. The changes in temperature and pressure for each simulation are then plotted and compared. The results of the simulations are summarized below in Table 5.1 and are discussed in the following text.

For Case A, loss of cooling on the condenser can result from a mechanical failure of the cooling water booster pumps or a loss of power to the pumps. If the vacuum is provided by a vacuum pump, mechanical failure or loss of power might lead to Case B as well. For the purpose of this work, the simultaneous loss of both (A) and (B) is not considered although with little effort, the model could also predict the consequences from a double failure.

The maximum heat input (Case C) is limited to five times the normal heat duty of the reboiler. The maximum heat case represents a number of possible realistic failures. For example, maximum heat could result from the full flow of steam from a header or even from a pool fire under the column.

For the simulation runs that use a quench stream, the quench stream is a cold (30 C) acetic anhydride stream fed at a rate of 10 gpm not to exceed 200 gallons. For the simulation runs that explore a dump scenario, the dump stream is based on gravity flow of the column contents at a rate of 10 gpm.

In Runs #1, #2, and #3, the cooling water is lost to the condenser. The vacuum system remains operational. The simulation results are shown in Figures 5.3, 5.4, and 5.5 on page 56. Within 6 minutes, the temperature in the base of the column reaches the trip temperature (T1) and activates the emergency shutdown logic. The steam flow (Q_R)

Table 5.1: Failure Analysis Summary for Refining Column Simulation

Initiation			Actions Taken						Results		
Run #	Failure Mode	ESD Trip Temp (C)	Stop Steam	Stop Feed	Stop UF	Break Vac	Quench	Dump	Time to ESD (min)	Max. DP Rise (torr)	Time to PSE opens (min)
1	loss cooling	T1	Y	Y	Y	N	N	N	6	660	n/a
2	loss cooling	T1	Y	Y	Y	N	Y	N	6	660	n/a
3	loss cooling	T1	Y	Y	N	N	N	Y	6	660	n/a
4	loss cooling	T2	Y	Y	Y	N	N	N	3	250	n/a
5	loss vacuum	T1	Y	Y	Y	N	N	N	17	1650**	36
6	loss vacuum	T1	Y	Y	N	N	Y	N	17	1650**	80
7	loss vacuum	T1	Y	Y	N	N	N	Y	17	1600	n/a
8	loss vacuum	T2	Y	Y	Y	N	N	N	12	1650**	240
9	loss vacuum	T2	Y	Y	Y	N	Y	N	12	1650**	930
10	loss vacuum	T2	Y	Y	N	N	N	Y	12	270	n/a
11	Max Ht Input	T1	Y	Y	Y	N	N	N	1.5	520	n/a
12	Max Ht Input	T2	Y	Y	Y	N	N	N	1	250	n/a

Notes: 1) T2 = T1 - 20 degrees C

2) Column rupture disks opens if the change in pressure >1650 Torr. Model cannot accurately predict pressure beyond this range because simulator lacks 2-phase flow capability

3) PSE = "pressure safety element" (i.e rupture disk)

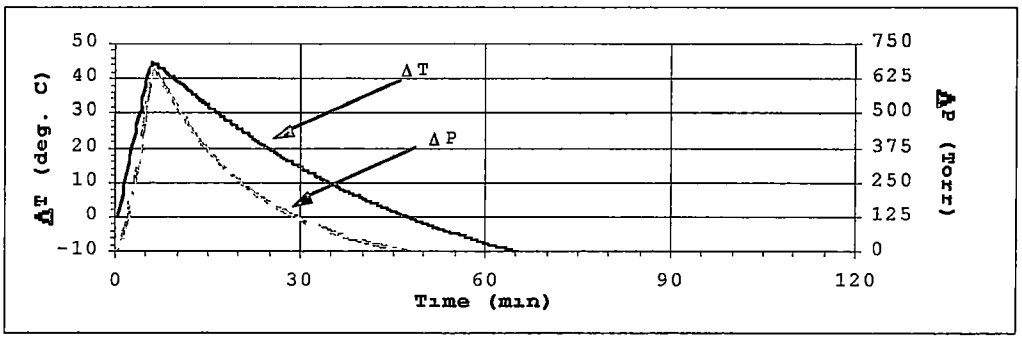

Figure 5.3: Simulation #1. The Change in the Temperature and Pressure in the Base of the Column After the Loss of Condenser Cooling and with only the ESD Active (Trip Temp. T1).

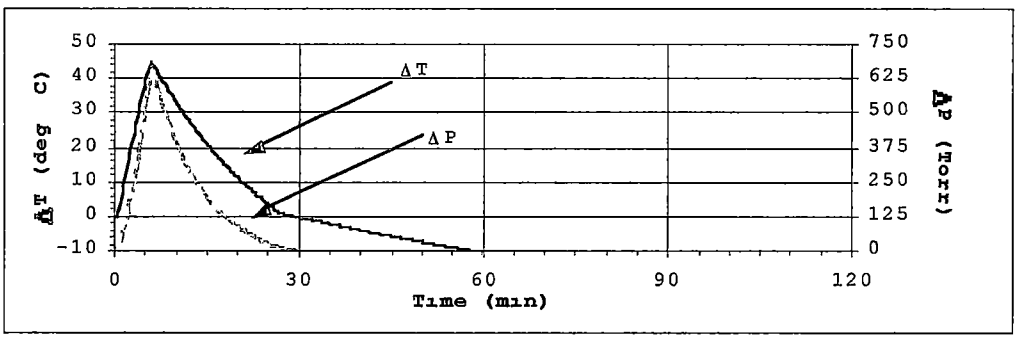

Figure 5.4: Simulation #2. The Change in the Temperature and Pressure in the Base of the Column After the Loss of Condenser and with the ESD Active (Trip Temp. T1) and a 10 gpm Quench.

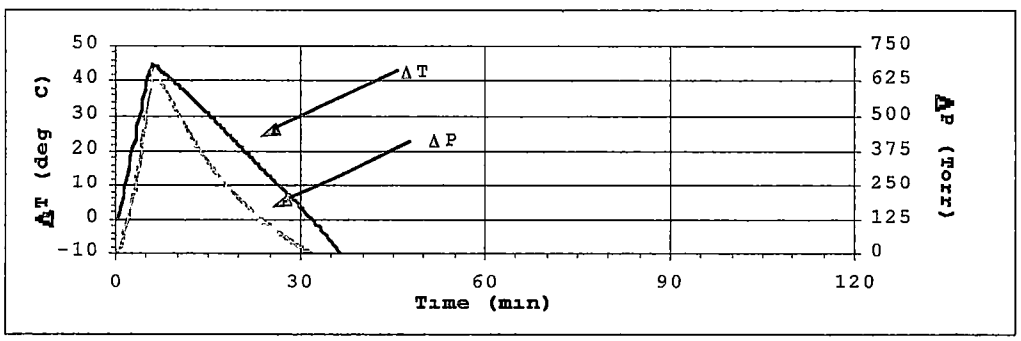

Figure 5.5: Simulation #3. The Change in the Temperature and Pressure in the Base of the Column After the Loss of Condenser Cooling and with the ESD System (Trip Temp. T1) and a 10 gpm Dump Stream.

and feed flow are immediately stopped and the column underflow valve is closed.

The ESD, by itself, performs very well and mitigates any danger. The maximum pressure never exceeds the pressure at which the hypothetical relief device will open. The addition of a quench and dump system provide no significant benefit over the emergency shutdown strategy by itself. However, a substantial improvement in the response is seen when the interlock trip temperature is reduced by 20°C as in Run #4 (see Figure 5.6). The maximum pressure the column reaches is half that observed in Run #1.

For Runs #5, #6, and #7, the vacuum system fails (see Figures 5.7, 5.8, and 5.9 on page 58). Although the column condenser remains operational, the condenser is constrained and cannot remove enough heat to temper the reaction. After approximately 17 minutes, the base temperature rises to T1 and activates the ESD, quench steam, or dump systems, respectively.

With the high ESD initiation temperature (T1), none of the emergency responses can prevent the column rupture disk from bursting. The column temperature decreases initially but then continues to rise as the reaction proceeds and generates more non-condensable gases. In

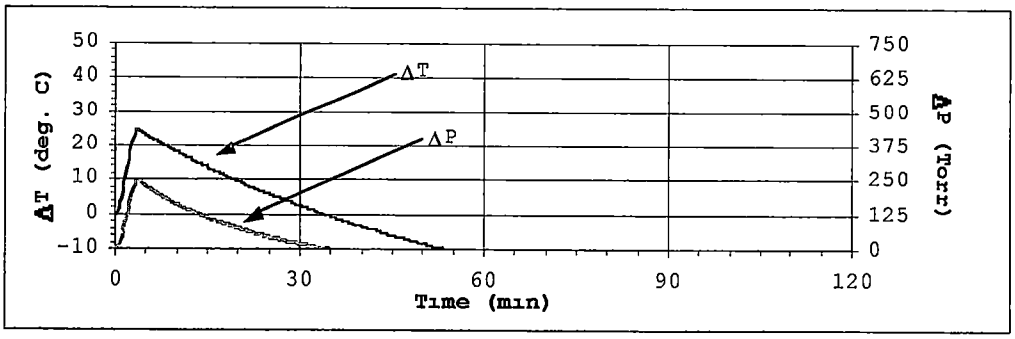

Figure 5.6: Simulation #4. The Change in the Temperature and Pressure in the Base of the Column After the Loss of Condenser Cooling and with only the ESD Active (Trip Temp. T2).

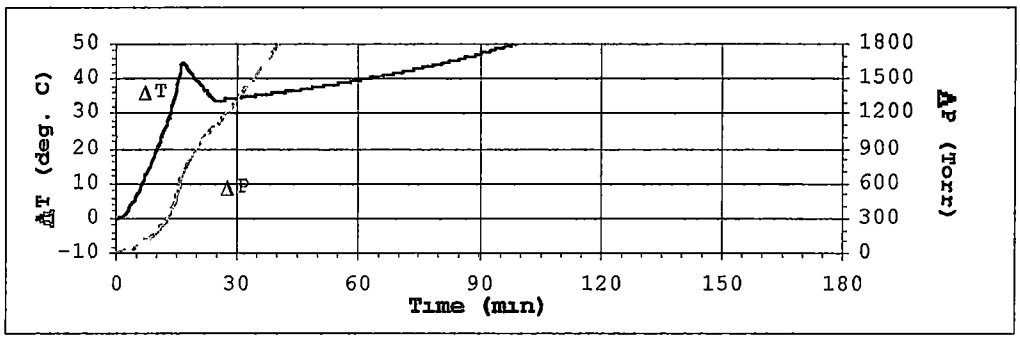

Figure 5.7: Simulation #5. The Change in the Temperature and Pressure in the Base of the Column After the Loss of Vacuum System and with only the ESD Active (Trip Temp. T1).

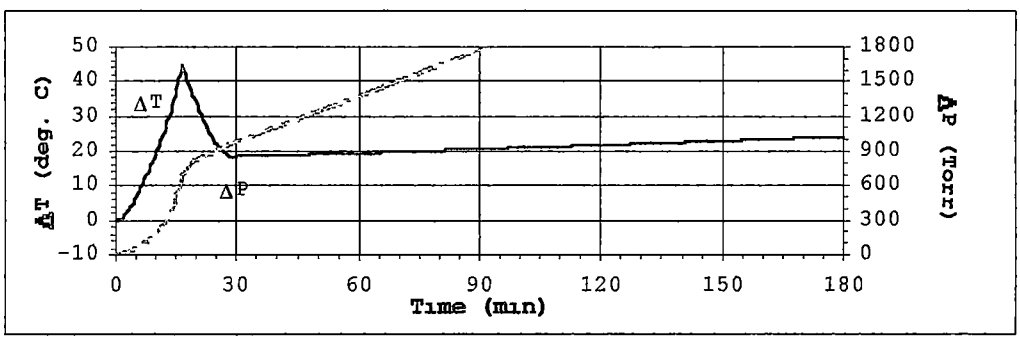

Figure 5.8: Simulation #6. The Change in the Temperature and Pressure in the Base of the Column After the Loss of Vacuum System and with the ESD (Trip Temp. T1) and a 10 gpm Quench.

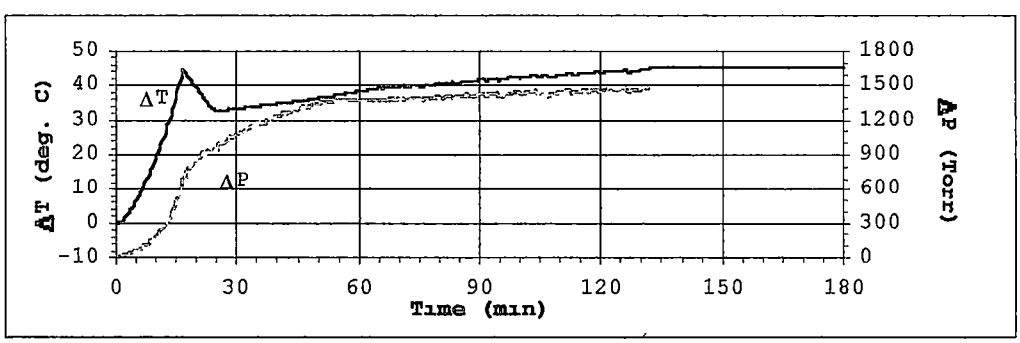

Figure 5.9: Simulation #7. The Change in the Temperature and Pressure in the Base of the Column After the Loss of Vacuum System and with only the ESD Active (Trip Temp. T1) and a 10 gpm Dump Stream.

two of three runs, the maximum pressure corresponds to the point at which the relief device opens. In Run #7, the maximum pressure corresponds with the depletion of the column inventory. If the model contained a few more gallons of liquid, the maximum pressure might also exceed the relief pressure setting.

The increase in pressure is more dramatic than the increase in temperature. The reason for this is that the pressure results from the rapid generation of non-condensable gases in a small vapor space. The liquid temperature rises more slowly because of the inertia of the large liquid inventory.

When vacuum is lost but the trip temperature is 20°C less (T2), the pressure rises at a much slower rate (see Figures 5.10, 5.11, and 5.12 on page 60). For Run #8, the computer simulation predicts the rupture disk will burst in 6 hours as opposed to 0.5 hours for the higher trip temperature. In Run #9, the quench system does not prevent the column rupture disk from bursting although it drastically slows the time until release from 6 to 15.5 hours. The dump strategy provides the most promise. If activated at sufficiently low temperatures, this option may prevent a vapor release.

For the case in which excess heat is added to the column as in Runs #11 and #12, the ESD automatically closes the steam supply valve (see Figures 5.13 and 5.14 on page 61). The ESD strategy performs very well in this case. The base temperature rises to T1 in 1.5 minutes and activates the ESD. But the maximum pressure never exceeds the relief pressure setting.

In Run #12, the maximum heat duty is again simulated as in Run #11. However, the initiation temperature is reduced by 20°C (T2). The lower trip value reduces the maximum pressure to two-thirds that seen in Run #11.

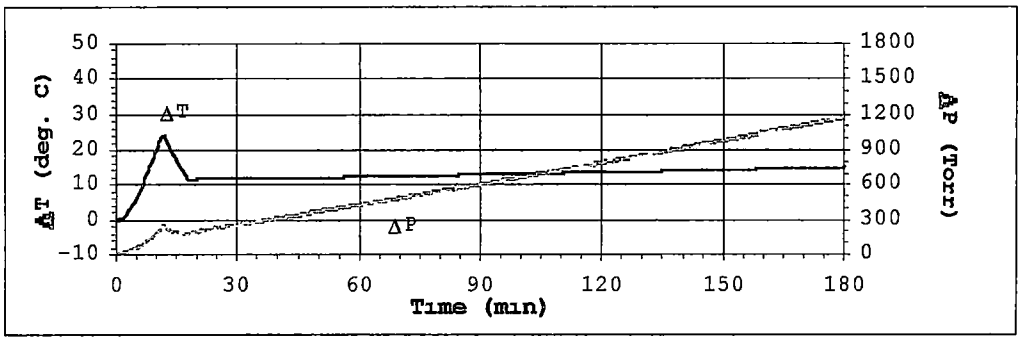

Figure 5.10: Simulation #8. The Change in the Temperature and Pressure in the Base of the Column After the Loss of Vacuum and with only the ESD Active (Trip Temp. T2).

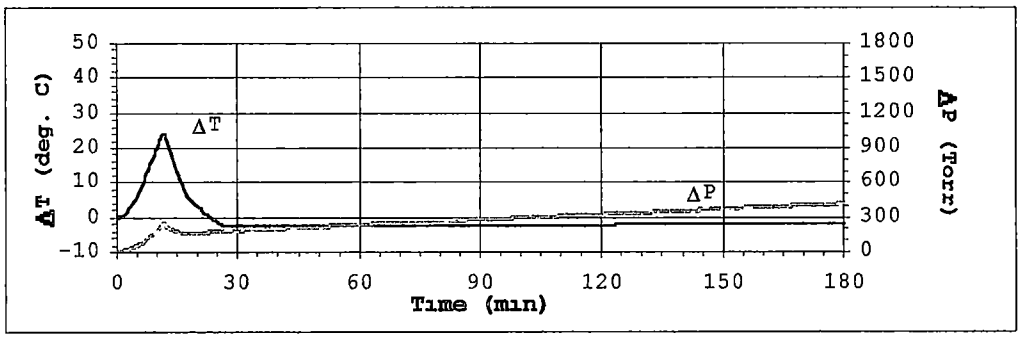

Figure 5.11: Simulation #9. The Change in the Temperature and Pressure in the Base of the Column After the Loss of Vacuum System and with the ESD Active (Trip Temp. T2) and a 10 gpm Quench.

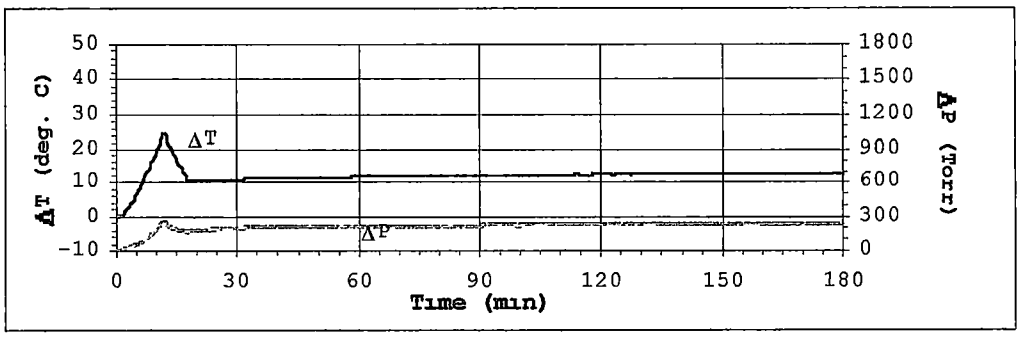

Figure 5.12: Simulation #10. The Change in the Temperature and Pressure in the Base of the Column After the Loss of Vacuum and with the ESD Active (Trip Temp. T2) and a 10 gpm Dump Stream.

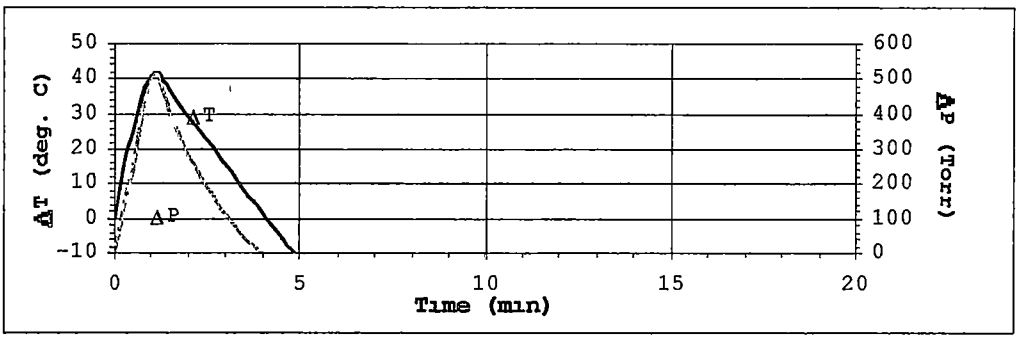

Figure 5.13: **Simulation #11. The Change in the Temperature and Pressure in the Base of the Column Upon Exposure to Excess Heat and with only the ESD Active (Trip Temp. T1).**

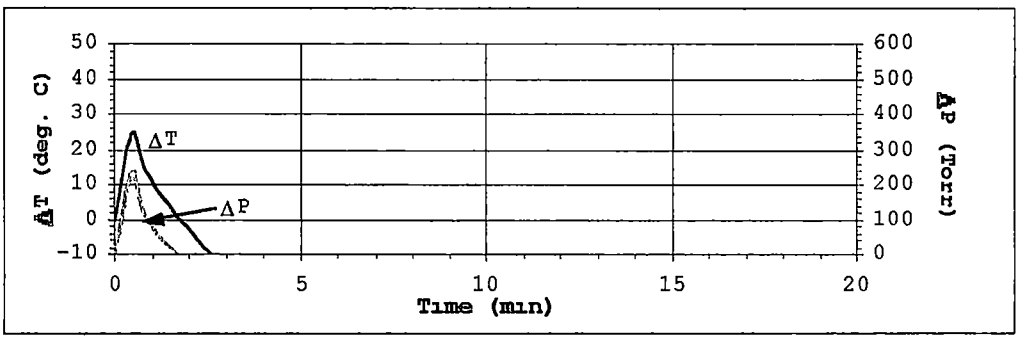

Figure 5.14: **Simulation #12. The Change in the Temperature and Pressure in the Base of the Column Upon Exposure to Excess Heat and with only the ESD Active (Trip Temp. T2).**

5.5 Discussion of Results

As noted earlier, the simulation provides conservative predictions of temperature and pressure rise from a runaway reaction of diketene. Based on the simulation results, the proposed emergency shutdown system performs very well in two of three failures tested. For loss of cooling and excess heat, the ESD initiation temperature (T1) and the actions taken by the ESD logic are adequate to prevent a violent runaway reaction.

However, the model suggests that high pressure in the column may still occur in the event vacuum is lost. For the conditions simulated, the pressure relief device will open to vent the column only 30 minutes after the vacuum is lost. This would be an undesirable scenario because diketene is a strong lachrymator and is highly flammable.

Reducing the ESD trip temperature (T_{ESD}) by 20°C greatly reduces the rate of pressure increase and limits the maximum overall pressure. This improvement is highly recommended to provide a greater margin of safety. Although the model predicts that loss of vacuum could still lead to over-pressurization, the time until the rupture disk (PSE) device opens is 6 hours as opposed to 0.5 hours with the current ESD trip temperature. This additional time may allow the operations forces time to restart the pump or to slowly bleed the column pressure to a safe location.

The addition of a quench system provides no major advantage in the safety response. On the other hand, the dump system can mitigate the loss of vacuum scenario. But as noted earlier, there are many concerns with a dump system including plugging of the dump valve or line. The term "dump" normally implies a large flow rate. However, as modeled, the dump stream is relatively small (10 gpm) and represents a reasonable maximum flow through the normal column underflow line. Assuming the underflow pump is still functioning, the "dump" need be nothing more than using the normal column underflow

line to de-inventory the column. More simply stated, if vacuum is lost and the ESD is activated, the underflow valve should open rather than close.

It should also be noted that different conditions of the dump and quench systems may lead to different conclusion. For example, if a 100 gpm quench stream is used instead of 10 gpm, the quench might provide better response. Similarly, if the dump system operates by gravity and cannot physically attain the 10-gpm flow, then the dump system might not mitigate the vacuum case at all. The advantage of dynamic simulation is that these variations can be modeled quickly and safely to ensure the proper safety system is selected.

CHAPTER 6

CONCLUSIONS AND RECOMMENDATIONS FOR FUTURE STUDY

6.1 Conclusions

This work demonstrates the effectiveness of using calorimetric testing and dynamic simulation to predict and control violently reactive chemical reactions. The Accelerated Rate Calorimeter is a beneficial tool in the development of the reaction kinetics. Computer models are useful not only to validate the reaction model, but also to simulate the reaction behavior in an industrial chemical process. This combination of laboratory and digital technology allows engineers to determine the safe operating limits for new chemical processes and design suitable emergency safety systems that may prevent future disasters.

For the hypothetical diketene refining process, the dynamic simulation shows that the current emergency shutdown strategy provides adequate safety response for two of the potential failure modes. However, significant safety improvements can be obtained by reducing the temperature initiation by 20°C. The margin of safety can be further improved by de-inventorying the column to a safe location by either automated logic sequence or manual intervention. Quenching provides no real advantages for this scenario.

The computer simulation also shows that in most cases, the column pressure safety device will not open. Therefore, an environmental release would not likely occur. In the event the relief device must open, the improvements in the emergency shutdown logic should reduce the amount of energy and vapors that may be released to the environment.

6.2 Recommendations for Future Study

The use of computer modeling for runaway reactions is becoming more widely used. However, such modeling is time consuming and laboratory testing to determine reaction parameters is expensive. Furthermore, only a few of the commercially available dynamic simulator software packages currently used have the capability to model two-phase vapor-liquid flow through nozzles and pipes. One such package is SAFIRE (Systems Analysis for Integrated Relief Evaluation) from Fauske and Associates, Inc. Unfortunately, this package is primarily designed for rating relief valve/rupture disks and is not ideal for testing other emergency response options.

Integration of two-phase vapor liquid flow subroutines into the dynamic modeling software can provide an even more powerful tool for the assessment of runaway reaction behavior. This software could be used not only to rate or design relief devices, but also to test emergency shutdown strategies, inhibitor dosing systems, and design effluent handling systems, etc.

LIST OF REFERENCES

Agreda, V.H. and J.R. Zoeller (ed.), *Acetic Acid and Its Derivatives*. 1993, New York: Marcel Drekkar, Inc.

Becker, M.L., S.S. Grossel, H.E. Huckins, and J.E. Huff, *Guidelines for Pressure Relief and Effluent Handling Systems*. 1998, New York: American Institute of Chemical Engineers

Bergmin, R, W. Quittmann, and J. Stoffel, U.S. Patent 4,999,468, Mar. 1991.

Bianchi, D., L. Rivolta, and V. Tartari, *Influenza dell'acido acetico sulla stabilita del dichetene*. Giornale di chimical industriale ed applicata L'industria chimica, 1985. **67**(5): p.245-249.

Clemens, R.J., *Diketene*. Chemical Reviews, 1986. **86**(2): p.241-318.

Fauske, H.K., H.G. Fisher, and J.C. Leung, *Thermal Runaway Reactions in a Low Thermal Inertia Apparatus*. Thermochimica Acta, 1986. **104**: p. 13-29.

Fisher, H.G., H.S. Forrest, S.S. Grossel, J.E. Huff, A.R. Muller, J.A. Norhonha, D.A. Shaw, and B.J. Tilley, *Emergency Relief System Design Using DIERS Technology*. 1992, New York: American Institute of Chemical Engineers.

Fuller, D.W., *Gas Evolution Rates from Diketene Decomposition*. 1984, Tennessee Eastman Company Technical Report No. TEAD-R-DC-84-706-2129.

Green, D.W. (ed.), *Perry's Chemical Engineers' Handbook*. 6th ed. 1984, New York: McGraw-Hill, Inc.

Huff, J. E., *Emergency Venting Requirements*. Plant/Operations Progress, 1982. **1**(4): p 211-229.

Jones, D.K., *1996 Update of the DIPPR Project 801 Database*. 1996, Eastman Chemical Company Research Report No. 96-1000-502

Lopatin, E.B., V.V. Popov, N.A. Epshtein, L.M. Mikhaleva, and Y.N. Makarov, *Kinetic and Thermochemical Characteristics of Diketene-Based Reactions*. Khimiko-Farmatsertícheskii Zhurnal, 1992. **26**(6): p.76-78.

Lunghi, A., M. Cattaneo, and P. Cardillo, *Explosion During Distillation in a Solvent Recovery Plant*. reprinted in Journal for Loss Prevention in the Process Industries, 1998. **11**: p.249-252.

Mansson, M., Y. Nakase, and S. Sunner, *The Enthalpies of Combustion and Formation of Diketene*. Acta Chemica Scandinavica, 1968. **22**: p.171-174.

Miller, R., C. Abaecherli, and A. Said, *Ketenes*. Ullman's Encyclopedia of Industrial Chemicals, 1990. **A15**: p. 63-76.

Townsend, D.I. and J.C. Tou, *Thermal Hazard Evaluation by an Accelerating Rate Calorimeter*. Thermochimica Acta, 1980. **37**: p. 1-30.

APPENDICES

APPENDIX A

DATA FOR REFINING COLUMN SIMULATION

Column specifications, reaction data, physical properties, and vapor-liquid equilibrium parameters are provided below. To abbreviate the text, the chemical compounds are identified as shown below. The physical property data for diketene is estimated (Jones, 1996).

Reference	Compound	Structure	Mol. Wt.
A	Diketene	$C_4H_4O_2$	84.08
B	Acetone	C_3H_6O	58.08
C	Acetic Acid	$C_2H_4O_2$	60.05
D	Acetic Anhydride	$C_4H_6O_3$	102.09
E	Water	H_2O	18.02
F	Carbon dioxide	CO_2	44.01
G	Carbon	C	12.01
H	Carbon monoxide	CO	28.01

I. Column Parameters

Column is modeled as two independent flash tanks representing the holdup in the top section and bottom sections of the column including the reboiler.

Crude Feed Flow	10 gpm
Quench Stream Flow	10 gpm (where used)
Dump Stream Flow	10 gpm (where used)
Residence Time in Base	35 min
Vapor Void Fraction in Base	30%
Residence Time in Top	15 min
Vapor Void Fraction in Top	75%
Maximum condenser duty	1.1 x $Q_{c,normal}$
Maximum reboiler duty	5 x $Q_{r,normal}$

II. Reaction Data

Reaction 1: $C_4H_4O_2$ (*l*) ⟶ 3 C(*s*) + H_2O (*l*) + C_3H_8O (*l*) + CO (*g*)

Reaction 2: $C_4H_4O_2$ (*l*) + H_2O (*l*) ⟶ CO_2 (*g*) + C_3H_8O (*l*)

Reaction takes place in the liquid phase

Rate Constants: $K_{for1} = 3 \times 10^{12} * e^{(-24000/RT)}$

$K_{for2} = 1 \times 10^{12} * e^{(-24000/RT)}$

[R = 1.987 cal/(gmol K), T in K]

Reaction Rate: (1) $K_{for} C_A$

(2) K_{for}

[lbmol/(hr ft^3), C_x in lbmol/ft^3]

Heat of Reaction: (1) -42,000 BTU/lbmol Diketene consumed

(2) -52,000 BTU/lbmol Water consumed

III. Physical Property Data

Liquid Molar Volume (cc/gmol):

A	79.78
B	73.17
C	55.83
D	92.46
E	18.07
F	37.27
G	7.46
H	35.44

Vapor Pressure [Torr, $P_i = \exp(A_{vpi} + B_{vpi}/(T + C_{vpi})$, T in °C]:

	A_{vpi}	B_{vpi}	C_{vpi}
A	18.26	-4153.0	230.0
B	16.65	-2941.0	237.2
C	16.81	-3404.0	216.8
D	17.45	-3931.0	223.5
E	18.33	-3842.0	228.3
F	13.63	- 164.9	276.3
G	18.51	-5885.0	226.2
H	13.63	0.0	0.0

Heat of Vaporization [BTU/lb, $\Delta H_i = A_{vi} + B_{vi}*T + C_{vi}*T^2 + C_{vi}*T^3$, T in °C]:

	A_{vi}	B_{vi}	C_{vi}	D_{vi}
A	225.30	-0.191	-1.57E-5	0.0
B	236.60	-0.247	-1.29E-3	0.0
C	161.20	0.198	-9.83E-4	0.0
D	200.00	-0.133	-1.02E-3	0.0
E	1068.0	-0.810	-8.62E-4	-4.57E-6
F	1.0	0.0	0.0	0.0
G	173.0	-.146	1.90E-4	0.0
H	99.53	0.0	0.0	0.0

Liquid Heat Capacity [BTU/lb °F, $h_l = A_{li} + B_{li}*T + C_{li}*T^2 + D_{li}*T^3$, T in °C]:

	A_{li}	B_{li}	C_{li}	D_l
A	0.787	8.78E-4	0.0	0.0
B	0.495	9.44E-4	0.0	0.0
C	0.467	4.00E-4	0.0	0.0
D	0.428	2.72E-4	2.98E-6	-4.65E-9
E	1.006	-3.27E-4	3.72E-6	-2.97E-9
F	0.226	0.0	0.0	0.0
G	0.337	3.93E-4	9.37E-7	0.0
H	0.226	0.0	0.0	0.0

Ideal Gas Heat Capacity [BTU/lb °F, $h_l = A_{li} + B_{li}*T + C_{li}*T^2$, T in °C]:

	A_{li}	B_{li}	C_{li}	D_l
A	0.297	0.0	0.0	0.0
B	0.362	7.34E-4	-1.51E-6	0.0
C	0.302	0.0	0.0	0.0
D	0.285	0.0	0.0	0.0
E	0.444	4.76E-6	2.56E-7	0.0
F	0.221	0.0	0.0	0.0
G	0.414	2.87E-6	-1.18E-8	0.0
H	0.249	1.90E-6	1.01E-7	0.0

IV. Vapor-Liquid Equilibrium Data

Wilson Parameters, given in terms of A_{ij}s, where

$$\ln \gamma_i = 1 - \ln\left(\sum_j x_j A_{ij}\right) - \sum_j \frac{x_j A_{ij}}{\sum_k x_k A_{kj}}$$

Component j \ Component i	A	B	C	D	E	F	G	H
A	1.0000	0.6354	0.8355	0.2979	1.0000	0.8155	1.0000	1.0000
B	1.0420	1.0000	2.5096	1.4550	1.0000	0.8346	1.0000	1.0000
C	0.5847	0.0511	1.0000	0 5499	1.0000	0.8974	1.0000	1.0000
D	1.6585	0.5238	0.9826	1.0000	1.0000	0.7839	1.0000	1 0000
E	1.0000	1.0000	1.0000	1.0000	1.0000	1.0000	1.0000	1.0000
F	1.2262	1.1981	1.1144	1.2757	1.0000	1.0000	1.0000	1.0000
G	1.0000	1.0000	1.0000	1 0000	1.0000	1.0000	1.0000	1.0000
H	1.0000	1.0000	1.0000	1.0000	1.0000	1.0000	1.0000	1.0000

Temperature of Conversion = 100 C

VITA

Heather McNabb was born Heather Maitland Leigh in Brevard, North Carolina on March 18, 1969. She graduated Salutatorian in 1987 from Berea High School in Greenville, South Carolina. The following September, she entered Clemson University in South Carolina. In 1992, she graduated Magna Cum Laude and received a Bachelor of Science degree in Chemical Engineering.

In June 1992, she accepted a position with Eastman Chemical Company in Kingsport, Tennessee. She worked for 3 years under the direction of Dr. James Downs in the Advanced Control Technology Group. This was followed by a 3-year appointment as Project Engineer for Eastman International Management Company's Latin America region. For three years, Heather worked closely with an international contract-engineering firm in the development, approval, and issuance of engineering deliverables. She has also served two years as a Process Safety Engineer in Eastman's Kingsport, Tennessee facility and is currently a Senior Development Chemical Engineer in the Global Polyester Polymers Technology Group.

In 1993, Heather began work toward a graduate degree in Chemical Engineering via the University of Tennessee Distance Learning program. In 1995, Heather's efforts to earn a graduate degree were temporarily postponed when she accepted an appointment as Project Engineer for the construction of a new plastics manufacturing facility in Argentina. In 1998 when she returned to the United States, Heather resumed her efforts to earn a graduate degree. In December of 2000, she completed her graduate work and received Master of Science degree in Chemical Engineering. Heather is also a registered Professional Engineer in the State of Tennessee.

Heather has been married since November 1992 to Kenney Wayne McNabb, a 1988 electrical engineering graduate of The University of Tennessee.